N83-30336

IO: ESCAPE AND IONIZATION OF ATMOSPHERIC GASES

Annual Report for Period
April 15, 1982 to April 14, 1983

Prepared for

NASA Headquarters
Washington, DC 20546

Prepared by

William H. Smyth
Atmospheric and Environmental Research, Inc.
840 Memorial Drive
Cambridge, Massachusetts 02139

TECHNICAL REPORT STANDARD TITLE PAGE

1. Report No. TWO	2. Government Accession No.	3. Recipient's Catalog No.
4. Title and Subtitle: Io Escape and Ionization of Atmospheric Gases		5. Report Date: April 1983 6. Performing Organization Code
7. Author(s): William H. Smyth		8. Performing Organization Report No.
9. Performing Organization Name and Address: Atmospheric and Environmental Research, Inc. 840 Memorial Drive Cambridge, Massachusetts 02139		10. Work Unit No. 11. Contract or Grant No. NASW-3503
12. Sponsoring Agency Name and Address: NASA Headquarters Headquarters Contract Division Washington, DC 20546		13. Type of Report and Period Covered: Annual Report April 15, 1982 - April 14, 1983 14. Sponsoring Agency Code: HWC-2
15. Supplementary Notes		

16. Abstract

Exploratory model calculations for the Io atomic oxygen cloud have provided two-dimensional sky-plane intensities for the 6300 Å, 1304 Å and 880 Å lines, where volume excitation and ionization rates are determined by impact collisions with Io plasma torus electrons. Comparison of model results with observations at 6300 Å suggests an isotropic oxygen flux from Io of about 1.5×10^9 atoms cm^{-2} sec^{-1}. The effects of including a neutral sulfur cloud and also of including charge exchange reactions between plasma torus ions and neutral OI and SI were evaluated to be significant and were roughly estimated to increase the required oxygen flux to 1.2×10^{10} atoms cm^{-2} sec^{-1}. In addition, increases in the estimates for the ion loading, cloud mass loss, plasma mass loading and ion energy input rates were also made. Model calculations for an Io sulfur cloud, excluding charge exchange reactions but assuming an SI flux of 7.5×10^8 atoms cm^{-2} sec^{-1} (i.e., half of the oxygen flux), were also performed and provided sky plane intensities for a number of visible and IR emission lines. In the analysis of the sodium cloud data, advances were reported which may prove to be important in determining the numerical basis functions suitable for proper model interpretation.

17. Key Words (Selected by Author(s))	18. Distribution Statement
satellite atmospheres planetary magnetospheres	

19. Security Classif. (of this report)	20. Security Classif. (of this page)	21. No. of Pages	22. Price*
unclassified	unclassified		

*For sale by the Clearinghouse for Federal Scientific and Technical Information, Springfield, Virginia 22151.

Figure 2. Technical Report Standard Title Page

I. INTRODUCTION

The nature of the local atmosphere of Io and the manner in which this atmosphere escapes to produce extended gas clouds and to supply the heavy ion plasma torus threading the satellite orbit are the central topics of this research. Io is known to have extended gas clouds of neutral sodium, potassium and oxygen detected by ground-based observations. In addition, detection of a neutral sulfur cloud has very recently been reported based upon UV emission data obtained from a rocket flight (Durrance, Feldman and Weaver, 1983). Io is also known to have a dense hot plasma torus composed primarily of oxygen and sulfur ions discovered by ground-based observers and more recently measured by instruments of the Voyager spacecrafts. The two basic goals of this research are to characterize the satellite emission conditions operative at Io for the sodium, oxygen and sulfur neutral gas clouds and to help characterize the satellite-ion source and magnetic diffusion of ions in the near Io environment.

To achieve the two research objectives, two different approaches are being followed. The first is to identify the atom escape characteristics of sodium from the satellite by analysis of the substantial neutral sodium cloud data base that has been obtained from Earth-telescope observations over the past ten years. The second is to explore by modeling analysis the implications of the rather recently discovered Io oxygen cloud (Brown, 1981) and the very recently reported detection of an Io sulfur cloud (Durrance, Feldman and Weaver, 1983). The discovery of the oxygen cloud in 1981 provided the first direct link between the loss of local atmospheric gases form the satellite and the supply of O^+ ions to the plasma torus. The relative importance of direct ion escape (i.e., S^+, O^+, SO^+, SO_2^+, etc.) and ionization of neutral gas clouds (i.e., S, O, SO_2, etc.) as ion supply channels for the plasma torus is currently not known. Better definition of the net rate at which O^+ ions and S^+ ions are supplied by ionization of the neutral gas clouds has been one of the major thrusts of our research effort this year. In addition to this net plasma source, the neutral gas clouds have also recently been realized (Johnson and Strobel, 1982) to <u>directly</u> alter to a significant extent the relative abundance of the plasma torus ions through neutral-ion exchange

reactions. The spatial distributions of the neutral clouds are in turn controlled by loss processes involving collisional ionization and charge exchange reactions. This complex coupling between the Io plasma torus and the neutral clouds has been a subject of intense interest in our research effort this year.

Progress made toward our two research objectives in the second year of this endeavor is reported here. The analysis of the sodium data has received less emphasis than the exploratory modeling of the oxygen cloud. Significant advancement has however been made toward each objective and is discussed in the following section.

II. PROGRESS DURING THE SECOND YEAR

Introduction

The strategy adopted during the second year has been to focus more effort upon the exploratory modeling of the Io atomic oxygen and atomic sulfur clouds and less effort upon the analysis of the Io sodium cloud data. This strategy was adopted to optimize our scientific program in response to reduced budgetary support. The sodium data analysis effort has thus been restricted to acquisition of new data and to determination of suitable modeling basis functions. Quantitative analysis of the sodium data will be initiated in the third year. The three-year plan for our data analysis modeling is summarized in Table 1.

Modeling of the Io Oxygen Cloud

Model Calculations

Further exploratory model calculations for the oxygen cloud, incorporating improvements in the Io plasma torus electron data adopted during the first year, have been performed in the second year. The distribution of OI in the extended cloud was placed on an absolute scale by fixing the modeled 6300Å emission intensity to the observed value (Brown, 1981), and model predicted intensities for the OI 1304Å and 880Å emissions were below observed upper limit values (Moos and Clarke, 1981; Shemansky, 1981). The loss process controlling the neutral population in these calculations was ionization by Io plasma torus electrons, and model results appropriate to the plasma conditions at the time of the Voyager 2 encounter with Jupiter are summarized in the second column of Table 2 (for more details see Smyth and Shemansky, 1983 included in the Appendix).

The effects of including a neutral sulfur cloud and also of including charge exchange reactions between plasma torus ions and the neutral OI and SI cloud atoms were evaluated and found to be significant. A rough estimate to include these effects was made by scaling (using as a guide the plasma torus calculations of Brown, Shemansky and Johnson, 1983) our Io oxygen cloud results (listed in the second column of Table

Table 1

Three-Year Plan for Data Analysis Modeling

Io Neutral Cloud Model	First Year	Second Year	Third Year
Oxygen	1. Add 1304Å and 880Å emission lines of OI to the model 2. Perform First Model Calculations (electron impact ionization only) 3. Improve Io plasma torus electron information	1. Perform further model calculations (electron impact ionization only) 2. Estimate effects of charge-exchange reactions and a sulfur cloud 3. Improve model to include oscillation of the plasma torus and charge-exchange reactions	1. Improve description of Io plasma torus in the models and improve model execution efficiency 2. Perform coupled Oxygen/Sulfur Model Calculations including oscillating torus electron impact ionization and charge-exchange reactions 3. Obtain and analyze model results for the neutral source fluxes, ion loading rates, ion diffusive loss time, plasma mass loading rate, satellite mass loss rate and ion energy input rate
Sulfur	Develop the Model	1. Perform first model calculations (electron impact ionization only) 2. Add new UV emission lines of SI to the model 3. Improve model to include oscillation of the plasma torus and charge-exchange reactions	
Sodium	Acquire and quality evaluate appropriate Earth-based data and supporting Voyager data	1. Begin model analysis for the line profile data 2. Initiate model analysis for select slit intensity data	1. Complete model analysis for the line profile data 2. Complete model analysis for the slit intensity data

Table 2

SUMMARY OF MODEL RESULTS

	Io Oxygen Cloud (electron impact ionization only)	Io Oxygen and Sulfur Cloud (charge exchange impact scaled)
1. Satellite Emission Flux:		
Oxygen	1.5×10^{9} atoms cm^{-2} sec^{-1}	1.2×10^{10} atoms cm^{-2} sec^{-1}
Sulfur	—	(6×10^{9} atoms cm^{-2} sec^{-1})
2. Ion Loading Rate (ion diffusive loss time)	6.2×10^{26} ions sec^{-1} (500 days)	~4×10^{27} ions sec^{-1} (~200 days)
3. Cloud Mass Loss Rate	16.6 kg sec^{-1}	~270 kg sec^{-1}
4. Plasma Mass Loading Rate	16.6 kg sec^{-1}	~150 kg sec^{-1}
5. Ion Energy Input Rate (% of torus UV energy budget)	2.7×10^{10} watts (~1%)	~4×10^{11} watts (~13%)

2) and assuming an Io sulfur flux of one-half the scaled oxygen flux. These scaled model results are summarized in the third column of Table 2 and are discussed in more detail by Smyth and Shemansky (1983). The ion loading, plasma mass loading and ion energy input rates, estimated in Table 2, strongly influence the composition, diffusion, field-aligned current systems and energy budget of the plasma torus and are of fundamental importance to models of the Jovian magnetosphere. The cloud mass loss rate, estimated in Table 2, is of fundamental importance in understanding the local atmosphere of Io and its interactions with the planetary magnetosphere. Obtaining a better estimate of these rates and their spatial character is therefore very important.

Model Improvements

Two major model improvements not included in the model results discussed above, were initiated in the latter part of the second year:

1. introduction of the oscillating motion of the plasma torus about the satellite plane, and
2. explicit inclusion of charge exchange reactions in the model, which affect both the cloud atom lifetime and the model predicted values of the physical rates listed in Table 2.

The first improvement has been implemented and most of the work required to implement the second improvement has been undertaken. To complete the second improvement, the spatial density of ions in the torus must be specified in two-dimensions. This information is at present only partially available. Parallel efforts have however been initiated to develop the necessary description of the ion densities in the plasma torus from the diverse and sometimes apparently contradictory sets of Earth-based, rocket, IUE, and Voyager measurements. Recent analysis of Voyager ion data by Bagenal (1983) has provided the required ion density information for the radial interval from 4.9 to 5.4 Jupiter radii. Additional information for the ion densities for larger radial displacements is also being sought from the analysis of Voyager UVS data by Shemansky (1983). The UVS inferred ion densities will be used to complement the Voyager ion data which does not uniquely define the ion densities in the hot torus (>5.7 Jupiter radii).

Charge exchange reaction rates for the model have been obtained from Johnson and Strobel (1982) and Johnson (1983). The set of relevant reactions adopted in the model are listed in Table 3 and the velocity dependence of the charge-exchange reaction rates have been included in the model as prescribed by Johnson (1983). Relevant electron impact ionization and recombination reactions are listed in Table 3 for the neutral species. Ion-ion and electron-ion reactions not producing neutral species as products are excluded from Table 3 since they are not required to calculate the model results in Table 2. Additional model results, such as the production or loss rate of a particular ion species, would however require these additional reactions to be incorporated. New model results will, in the near future, be limited to calculating improved values for only the rates listed in Table 2 (see the Appendix for further discussion).

Modeling of the Io Sulfur Cloud

Model Calculations

The Io sulfur cloud model, developed during the first year of the data analysis was used to calculate the intensity on the sky plane of electron impact excited emission lines at wavelengths of 11,306Å, 10,820Å, 7725Å and 4589Å. Model results for the stronger optical emission line at 7725Å are shown in Figure 1 for the same observational geometry used in the 6300Å oxygen model calculation (simulating the detection measurement of Brown in Figure 4 of the Appendix). The 7725Å intensity contours, in Rayleighs, are about an order of magnitude dimmer near Io than the 6300Å intensity contours for the oxygen cloud and are fixed by assuming a sulfur escape flux of one-half the value determined for the oxygen cloud. The sulfur cloud is more tightly confined near Io because its electron impact ionization lifetime shown in Figure 2 is about 4 to 5 times smaller than the electron impact ionization lifetime of oxygen (see Figure 3 in the Appendix). This is illustrated more clearly by comparison of the column density of both clouds as viewed from above the satellite plane in Figure 3.

Near Io, the intensity of the other optical line at 4589Å is about five times dimmer than the 7725Å line and therefore will not be

Table 3. Charge-Exchange and Electron Impact Reactions for Neutral Oxygen and Sulfur

	Reaction
1.	$O^+ + O \rightarrow O + O^+$
2.	$O^+ + S \rightarrow O(^3P) + S^+(^2P)$
	$\rightarrow O(^1D) + S^+(^2D)$
3.	$S^+ + S \rightarrow S + S^+$
4.	$S^+ + O \rightarrow S + O^+$
5.	$S^{++} + S \rightarrow S + S^{++}$
	$\rightarrow S^+(^4S) + S^+(3s, 3p^4; {}^4P)$
6.	$S^{++} + O \rightarrow S^+(^2P) + O^+(^2D)$
	$\rightarrow S^+(^2D) + O^+(^2D)$
	$\rightarrow S^+(^2D) + O^+(^2P)$
	$\rightarrow S^+(^4S) + O^+(^2P)$
7.	$O^{++} + O \rightarrow O + O^{++}$
	$\rightarrow O^+(^4S) + O^+(2s, 2p^4; {}^4P)$
	$\rightarrow O^+(^2D) + O^+(2s, 2p^4; {}^4P)$
8.	$O^{++} + S \rightarrow O^+(^4S) + (S^+)^*$
	$\rightarrow O^+(^2D) + (S^+)^*$
	$\rightarrow O^+(^2P) + (S^+)^*$
	$\rightarrow O(^2D^\circ\ 3d, {}^3P^\circ) + S^{++} \rightarrow O^+ + S^{++} + e$
9.	$S^{+++} + O \rightarrow S^{++}(3d, {}^3P) + O^+(^4S)$
	$\rightarrow S^{++}(4s, {}^3P) + O^+(^4S)$
	$\rightarrow S^+(^2P) + O^{++}(^3P)$
	$\rightarrow S^+(^2D) + O^{++}(^1D)$
	$\rightarrow S^+(^4S) + O^{++}(^1D)$
10.	$S^{+++} + S \rightarrow S^{++}(4p, {}^3D) + S^+(^4S)$
	$\rightarrow S^{++}(3d, {}^3P) + S^+(^2P)$
	$\rightarrow (S^{++})^* + S^+(^2D)$
	$\rightarrow (S^+)^* + S^{++}$
11.	$e + O \rightarrow O^+ + 2e$
12.	$e + S \rightarrow S^+ + 2e$
13.	$O^+ + e \rightarrow O + h\nu$
14.	$S^+ + e \rightarrow S + h\nu$

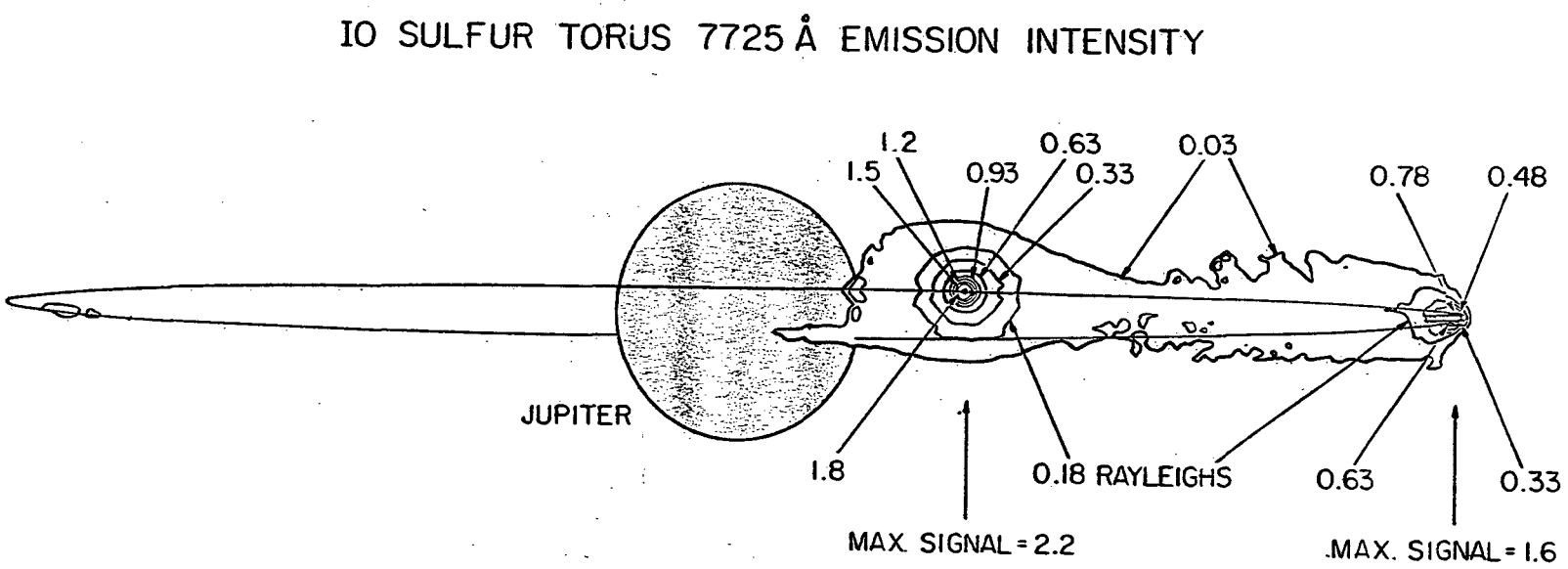

Figure 1. The satellite, its orbital path and the planet are shown in relation to the calculated intensity contours which assume an isotropic satellite flux of 7.5×10^8 sulfur atoms cm^{-2} sec^{-1} emitted radially from Io.

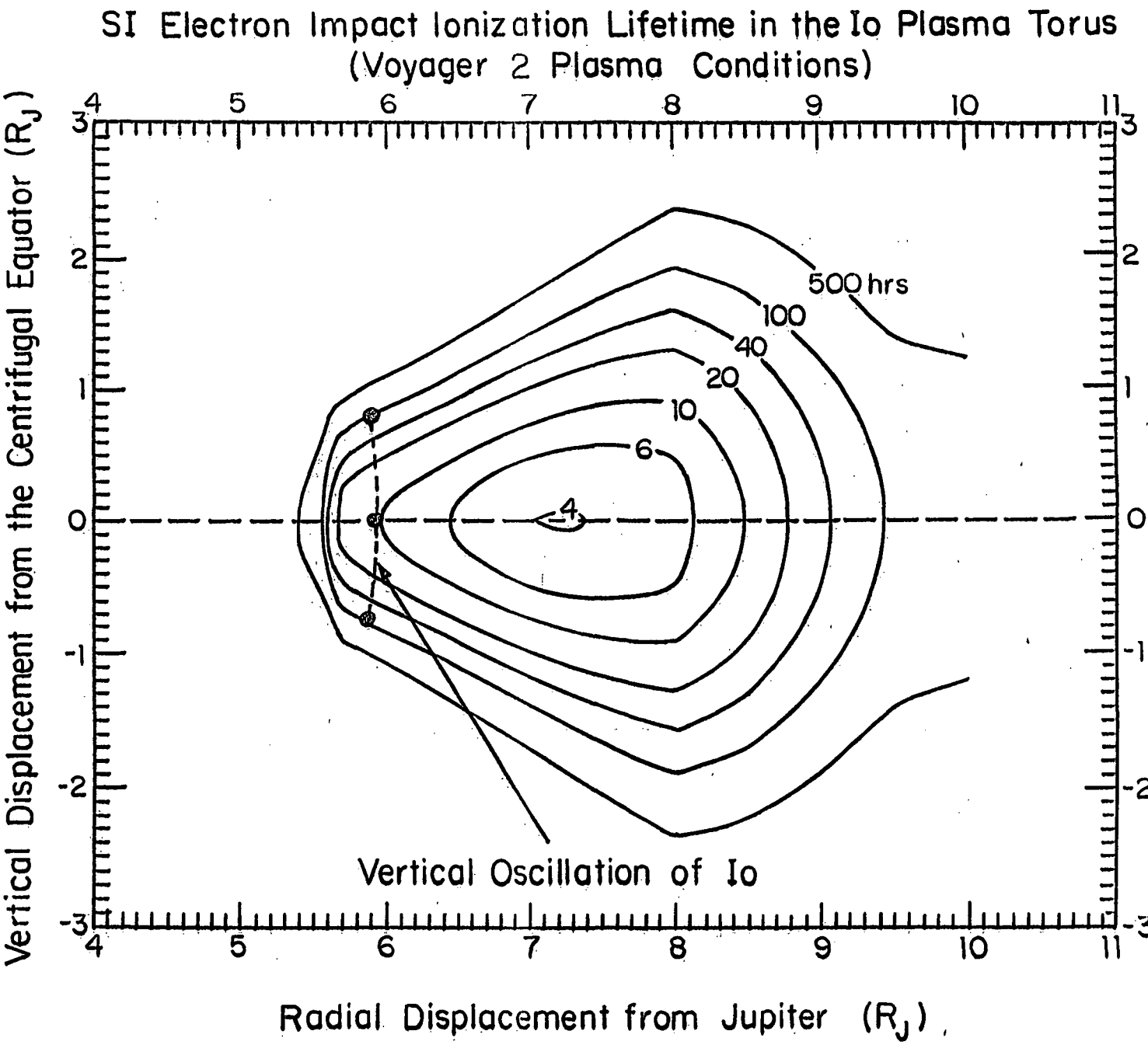

Figure 2. The lifetime is calculated using the plasma conditions adopted for the Voyager 2 encounter with Jupiter.

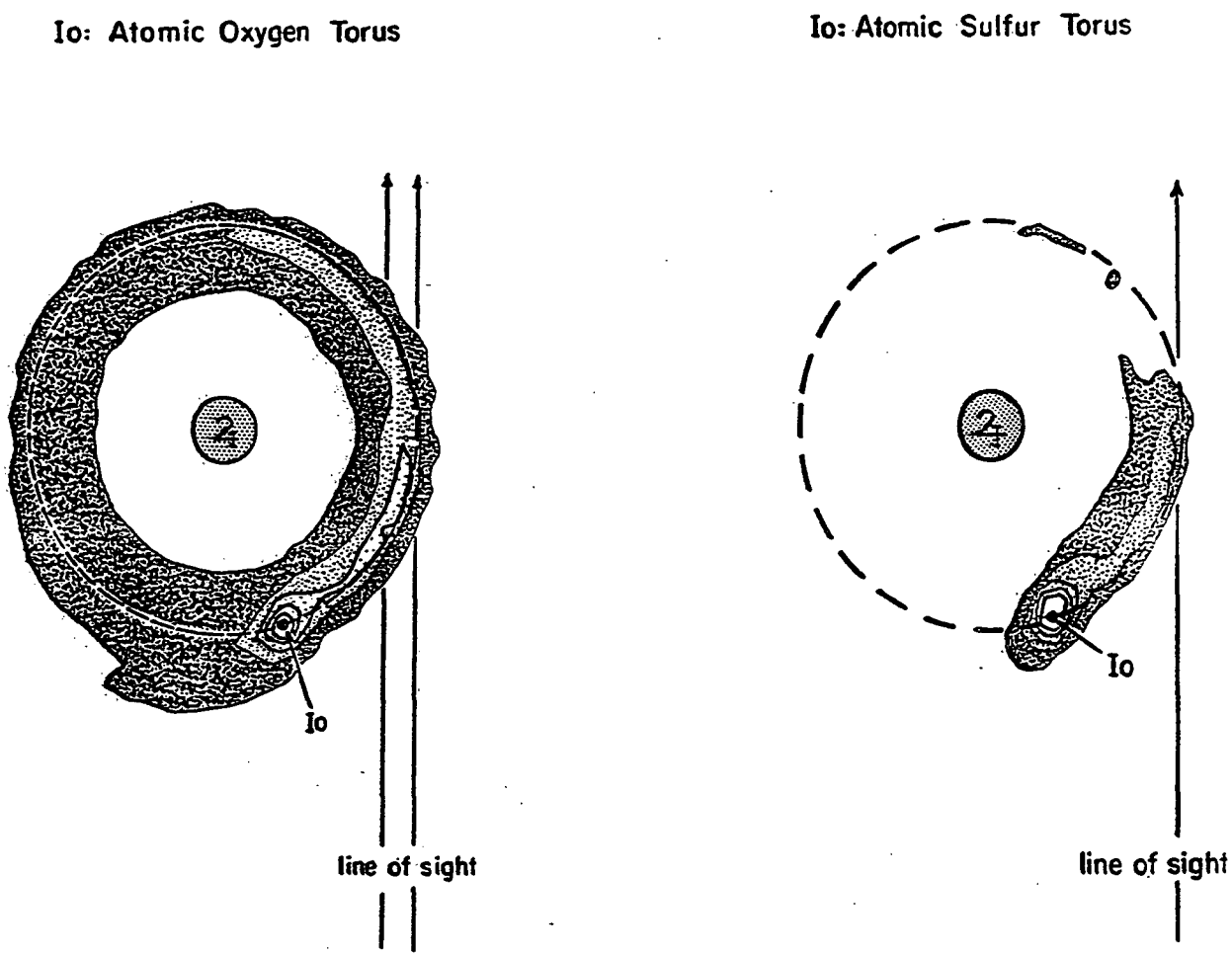

Figure 3. The column density morphology viewed from above the satellite orbit plane is calculated for the plasma conditions appropriate to the Voyager 2 encounter with Jupiter. The outer column density contours are comparable and correspond to an average dimensional density of about 1 atom cm^{-3}.

considered further. The IR line at 10,820Å is, however, comparable to the 6300Å oxygen line emission intensity near Io while the IR line at 11,306Å is about a factor of 3.5 dimmer. Comparable or brighter emission lines at UV wavelengths of 1304Å, 1425Å, 1485Å and 1820Å, also exist for neutral sulfur, as illustrated in Figure 4 for only one temperature of 80,000° K. The IR emission at 10,820Å provides the best line for ground-based detection of neutral sulfur while the UV emission at 1820Å provides the best line for rocket or Earth-orbiting satellite detection. Appropriate UV and IR observers have been notified of these emission lines and interest in observing the neutral sulfur cloud is growing.

Model Improvements

The model improvements discussed earlier for the oxygen cloud model have also been implemented for the sulfur cloud model. Progress parallels that achieved for the oxygen model. In addition, arrangements have been made with Shemansky (1983) to obtain approximate expressions for the electron emission rates for the UV lines of atomic sulfur listed above. Computations of the intensity of these UV emissions on the sky plane will be performed during the third year.

Analysis of the Io Sodium Cloud Data

The quantitative analysis of the Io sodium cloud data has been divided into five stages of activities which are summarized in Table 4. Due to the reduced budgetary support available, the original proposed scope of this data analysis modeling effort cannot be performed. A data set of more limited scope has therefore been selected with the overall goal of our modeling effort remaining unchanged. In order to retain the virtue of the analysis in step 4 and step 5, the limited data set will consist of both spectral data (the sodium line profile data) and some spatial intensity data (sodium D-line intensity variations on the sky plane as imaged through an observing slit). In the first year, efforts were directed to stage 1 activities of Table 1. Available line profile data [Trafton, 1975; Trauger, Roesler and Münch, 1976; Trauger, 1977; Trafton and Macy, 1977; Trafton, 1981] and spatial intensity data [Brown et al., 1975; Trafton and Macy, 1975;

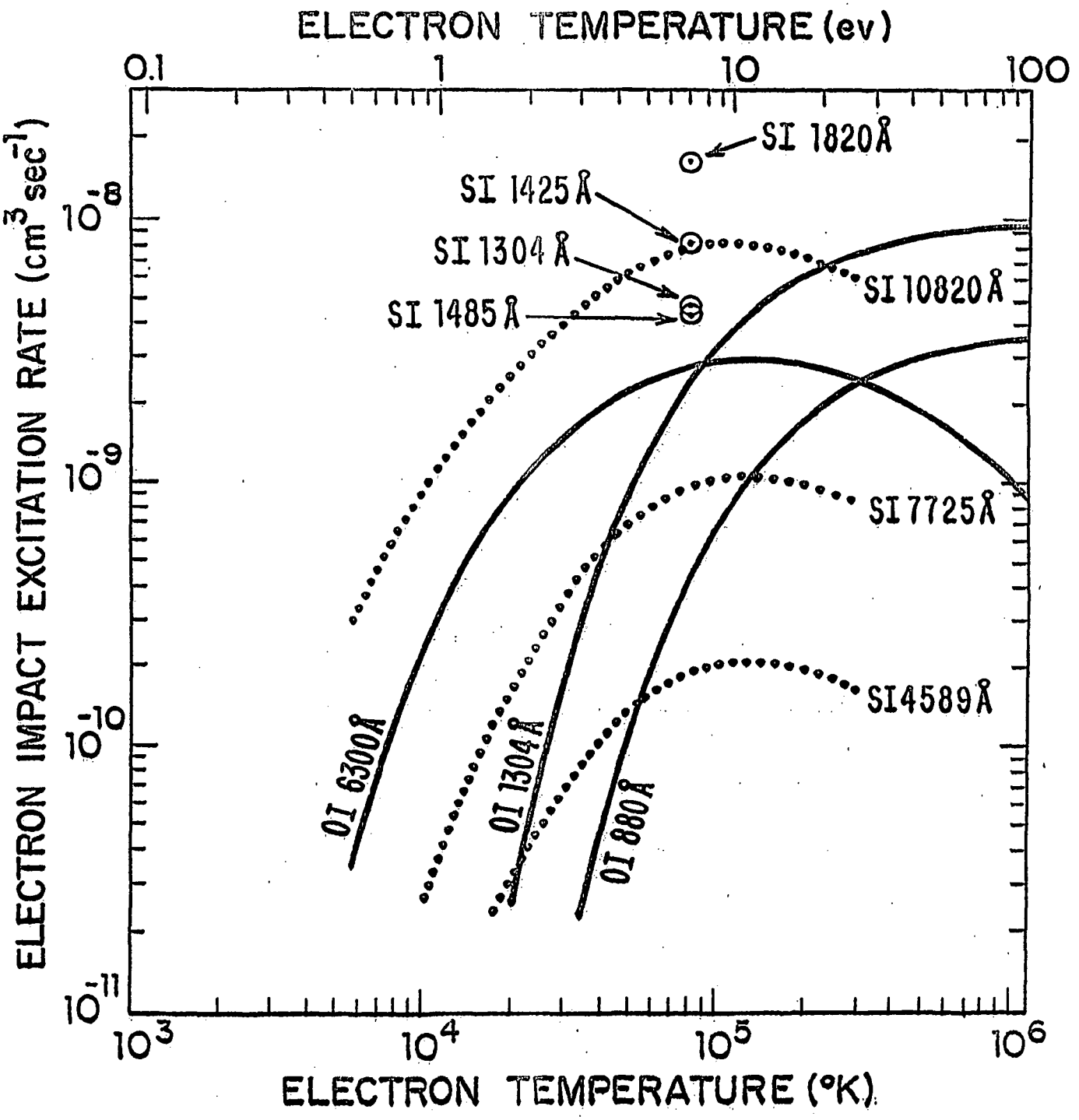

Figure 4. These electron impact excitation rate coefficients for neutral oxygen and sulfur were computed by Shemansky (1982). The visible and IR emission rates were based upon close coupling calculation taking into account configuration interactions that were performed by Henry (1981).

Table 4

Five Stages of the Quantitative Analysis of the Io Sodium Cloud Data

(1) acquiring and quality evaluation of the different Voyager and Earth-based data sets,

(2) performing suitable calculations using our highly developed numerical models to generate the appropriate (physical model parameter dependent) basis functions for analysis of selected observations,

(3) applying a simplex technique for non-linear optimization or at least squares technique with constraint optimization to each selected observation and its set of model basis functions for inversion and extraction of physical information,

(4) evaluating the compatibility of physical model parameters deduced from analysis of different observations, and

(5) performing consistent and simultaneous analysis of complementary data sets.

Trafton, 1977; Brown, 1977; Trafton and Macy, 1978; Mekler, 1982] were acquired and preliminarily evaluated. In the second year, efforts were directed to stage 2, with priority given to the line profile data.

The Io sodium cloud model, improved to include the space and time varying electron impact ionization sink of the oscillating plasma torus, will be used to generate the basis functions for analysis of the data set in the third year (steps 3-5). The purpose of the second-year effort (stage 2) has been to specify the physical model parameters (i.e., the exospheric escape conditions of sodium and the plasma torus sink conditions) sufficiently accurately so that the basis functions computed by the model are physically appropriate for data inversion. Improvements in the description of the electron density and temperature have been implemented in the model this year. Progress in selecting the exospheric escape conditions has resulted from (1) studying the character of the line profile data independent of the model and (2) applying new model results that have very recently become available from research performed in one of our other NASA supported projects (NASW-3387). The new model results and their implications for this project are briefly discussed below.

In our NASA supported research project (NASW-3387), modeling of the sodium directional features discovered by Pilcher (Hartline, 1980) has been in progress for the last three years. This modeling has recently resulted in the discovery of new and direct evidence for a magnetospheric-driven gas escape mechanism for Io. This modeling analysis has used the Io sodium cloud model with the oscillating plasma torus. It has shown that the directional features outside of Io's orbit can be understood in terms of (1) an oscillating plasma torus sink, (2) a high-velocity (~20 km sec^{-1}) sodium source whose direction must be nearly perpendicular to Io's orbital motion, and (3) a non-uniform flux of sodium from Io that is enhanced near the equator of the satellite. Adopting these exospheric escape conditions, preliminary efforts indicate that such high-velocity sodium atoms may also have the correct characteristics to explain the asymmetric skirt exhibited in the sodium line profile data. Basis functions consistent with these escape conditions will be evaluated more fully in the third year and may prove to eliminate past ambiguities that have existed in

choosing unique basis functions for data inversion of the line profile data. These escape conditions are also important in properly understanding the north-south alternating spatial intensity data [Trafton and Macy, 1975; Trafton, 1977] which comprises part of the complementary (i.e., non-spectral) information in our limited data set.

REFERENCES

Bagenal, F. (1983) Private communication.

Brown, R.A. (1977) Private communication.

Brown, R.A. (1981) The Jupiter hot plasma torus: Observed electron temperature and energy flow. Ap. J., 244, 1072.

Brown, R.A., Goody, R.M., Murcray, F.J. and Chaffee, F.H., Jr. (1975) Further studies of line emission from Io. Ap. J. Lett., 200, L49.

Brown, R.A., Shemansky, D.E. and Johnson, R.E. (1983) A deficiency of OIII in the Io plasma torus. Ap. J., 264, 309-323.

Durrance, S.T., Feldman, P.D. and Weaver, H.A. (1983) Rocket detection of ultraviolet emission from neutral oxygen and sulfur in the Io torus. Ap. J. Lett., 267, L125-L129.

Hartline, B.K. (1980) Voyager beguiled by Jovian Carrousel. Science, 208, 384.

Henry, R. (1981) Private communication with D.E. Shemansky.

Johnson, R.E. (1983) Private communication.

Johnson, R.E. and Strobel, D.F. (1982) Charge exchange in the Io torus and exosphere. J. Geophys. Res., 87, 10385.

Mekler, Y.B. (1982) Private communication.

Moos, H.W. and Clarke, J.T. (1981) Ultraviolet observations of the Io torus from the IUE observatory. Ap. J., 247, 354.

Pilcher, C.B., Smyth, W.H. and Combi, M.R. (1983) Article in preparation.

Shemansky, D.E. (1981) Private communication.

Shemansky, D.E. (1982) Private communication.

Shemansky, D.E. (1983) Private communication.

Smyth, W.H. and Shemansky, D.E. (1983) Escape and ionization of atomic oxygen from Io. Ap. J., August 15 issue.

Trafton, L. (1975) High-resolution spectra of Io's sodium emission. Ap. J., 202, L107.

Trafton, L. (1977) Periodic variations in Io's sodium and potassium clouds. Ap. J., 215, 960.

Trafton, L. (1981) Private communication.

Trafton, L. and Macy, W., Jr. (1975) An oscillating asymmetry to Io's sodium emission cloud. Ap. J. Lett., 202, L155.

Trafton, L. and Macy, W., Jr. (1977) Io's sodium emission profiles: Variations due to Io's phase and magnetic latitude. Ap. J., 215, 971.

Trafton, L. and Macy, W., Jr. (1978) On the distribution of sodium in the vicinity of Io. Icarus, 33, 322.

Trauger, J.T. (1977) Private communication.

Trauger, J.T., Roesler, F.L. and Münch, G. (1976) Velocity structure in the sodium emission from Io. Bull. AAS, 8, 468.

Escape and Ionization of Atomic Oxygen from Io

William H. Smyth

Atmospheric and Environmental Research, Inc.

Donald E. Shemansky

University of Southern California

Received 1982 August 11

Abstract

The escape of atomic oxygen from Io and its distribution in the magnetosphere of Jupiter is described in a model calculation. The loss process controlling the neutral population in this calculation is ionization by plasma electrons. The OI distribution is placed on an absolute scale by fixing the modeled 6300 Å emission intensity to the observed value. Predicted intensities for the OI 1304 Å, and 880 Å emissions are included in the calculation. The model indicates a satellite emission flux of 1.5×10^{9} cm^{-2} s^{-1}, an ion loading rate of 6.2×10^{26} ions s^{-1}, an oxygen ion mass loading rate of 16.6 kg s^{-1}, and an oxygen ion energy input rate of 2.7×10^{10} watts. The effect of including a neutral sulfur cloud and charge exchange reactions in the plasma torus is significant. A rough estimate including these effects raises the source flux for oxygen atoms to 1.2×10^{10} cm^{-2} s^{-1}. The inclusion of an assumed satellite flux for sulfur atoms of 6.0×10^{9} cm^{-2} s^{-1} then produces an ion loading rate of $\sim 4.0 \times 10^{27}$ ions s^{-1}, an ion diffusive loss time of ~200 days, a plasma mass loading rate of ~150 kg s^{-1}, a satellite mass loss rate of ~270 kg s^{-1}, and a maximum ion energy input of $\sim 4 \times 10^{11}$ watts. The energy lost by radiation (3×10^{12} W) from the Voyager 2 epoch plasma torus exceeds the estimated energy input through the production of new ions by an order of magnitude.

1. Introduction

Io, the innermost Galilean satellite of Jupiter, is known to be the source of a substantial plasma torus in the Jovian magnetosphere composed primarily of oxygen and sulfur ions. The satellite is also known to have neutral gas clouds extending spatially beyond its local gravitational control. To date, neutral gas clouds of sodium (Brown 1974), potassium (Trafton 1975; Münch, Trauger, and Roesler 1976; Trauger, Roesler, and Münch 1976) and atomic oxygen (Brown 1981) have been detected from ground-based facilities, and at least one other species, neutral sulfur, has now been reported as an observed emission by Durrance, Feldman, and Weaver (1982).

The role of the neutral gas clouds of Io as controlling factors for the maintenance and morphology of magnetospheric plasma has not been generally recognized. However, if mass is continuously lost from the plasma as it must be through various processes, neutral particles must ultimately serve as fodder for the maintenance of the system. If neutral clouds exist in the space of the plasma torus they must certainly be a source of new ions. The recent discovery of the atomic oxygen cloud in the plasma torus remote from Io (Brown 1981) demonstrates the presence of a significant source of both plasma and energetic neutral atoms for the magnetosphere because of the recent realization that neutral-ion charge exchange reactions in addition to electron collisions, are controlling factors in the Io plasma torus (Brown, Pilcher and Strobel 1983; Johnson and Strobel 1982; Brown, Shemansky, and Johnson 1983; Brown and Shemansky 1982). The action of these processes is such that the characteristics of the Io atomic oxygen cloud and the properties of the magnetosphere are strongly coupled.

The significance of the recent detection by Brown (1981) of an atomic cloud near the orbit of Io, achieved by observing its electron-excited

emission in the 6300 Å line, is that it provides us with the first direct information to link the escape of neutral gas from the satellite and the observed oxygen and sulfur ions in the plasma torus. The population of such neutral gas clouds in the Jovian circumplanetary space is governed by the source rate at Io and by the subsequent loss processes which occur for the escaping atoms along their orbital paths in the magnetosphere. The interaction of these clouds with the plasma torus forms the dominant sink, converting the atoms to ions in collision with electrons and existing ions. The observation of excited emission from the OI atoms through their collision with the torus plasma electrons can then provide a means of estimating both the neutral cloud density and the resulting mass, ion and energy input supplied to the magnetosphere by the cloud. Those quantities, which are fundamental to understanding the connection of the plasma torus to the magnetosphere, have been the subject of heated discussion in the literature. The torus mass loading and diffusive loss rates have been estimated by a variety of methods (Sullivan and Siscoe, 1981; Eviatar and Siscoe, 1980; Richardson et al., 1980; Richardson and Siscoe, 1981; Dessler, 1980; Brown, 1981; Shemansky, 1980; Thorne, 1981; Hill, 1980) providing values separated by factors of 100 or more. An uncritical reader of the various arguments therefore cannot arrive at a sensible conclusion in regard to questions relating to how energy is delivered to the torus for its maintenance, and the nature of the interaction of the torus with Jupiter's atmosphere and magnetosphere.

The emphasis of this article will be to explore what can be learned about the escape processes of atomic oxygen from Io and the plasma source that the neutral gas forms in the planetary magnetosphere. Other plasma sources for

the magnetosphere such as direct ion escape from Io, escape of molecules such as SO_2 followed by dissociation and ionization, or escape of molecular ions such as SO_2^+ followed by dissociative processes are also possible, but none of these processes have yet been positively identified. To explore the characteristics of the atomic oxygen cloud and its impact on the magnetosphere, a model for the gas cloud has been developed and suitable calculations performed.

The model calculation requires establishment of a reasonably accurate temperature and density structure for the plasma, which we obtain from a combination of Voyager in situ and EUV data. The loss process providing the sink for neutrals in this calculation is electron impact ionization only, although we realize that charge exchange reactions are an important additional loss process in some regions of the torus. However, pending further detailed calculations, we make rough estimates below of the effect of ion-atom reactions on the atomic oxygen distribution and source rates, based on recent work by Brown, Shemansky, and Johnson (1983).

Qualitatively the Brown (1981) observation of OI 6300 Å emission indicates a rather low abundance implying low mass loading and source rates compared to most of the earlier published results. The energy injection rate based on the calculated production rate of ions is too low to compensate for the known radiative cooling rate. This result is not new in the published literature since Shemansky (1980) and Shemansky and Sandel (1982) have obtained similar results based on other considerations. However there are conflicts with the other work indicated above, and the present results are by no means generally accepted. We present the model calculation below and cite the arguments and uncertainties in the issue.

2. Atomic Oxygen Cloud Model

Brown (1981) by adding six individual observed spectra obtained an intensity of 8±4 Rayleighs in the 6300 Å emission lines. This difficult detection, which required three hours of integration time, was made possible by the high spectral resolution of his instrument which separated the Io emission line from the bright telluric oxygen airglow line of approximately 80 Rayleighs. The Io related emission in the 6300 Å lines is excited by inelastic impact of oxygen atoms and Io plasma torus electrons (Brown, 1981). Other attempts to observe electron-impact excited emissions of the oxygen cloud at wavelengths of 1304 Å and 880 Å, summarized in Table 1 have provided only upper limits. The plasma torus in addition provides a sink for the Io atomic oxygen cloud through electron impact ionization and ion charge exchange reactions. The effect of charge exchange processes, although important in the dense regions of the hot torus near Io's orbit (Brown, Shemansky and Johnson, 1983) and in the inner cool region where the torus electrons become too cold for impact ionization (Johnson and Strobel, 1982) has not been included here as mentioned earlier. The brightness of the oxygen atom emission in a given volume element of the cloud is thus determined by the local electron number density and temperature, while the number of oxygen atoms in that volume element is determined by the previous ionization time-history of these atoms in the planetary environment and the source injection rate.

Modeling the density, 6300 Å, 1304 Å, and 880 Å emission intensities, and instantaneous oxygen ion creation rate of the oxygen cloud is achieved by following in circumplanetary space the trajectories of many oxygen atoms ejected from Io and by determining proper weights along these trajectories to reflect their real time volume excitation and ionization rates. The

trajectories in circumplanetary space from the assumed isotropic ejection process at Io are determined by solving the circular restricted three-body equations of motion for each atom with suitably specified initial conditions. This procedure has been documented in detail by Smyth and McElroy (1977 and 1978) who applied this method to modeling the Io sodium cloud. To determine the proper excitation and ionization weights along these trajectories, the volume excitation and ionization rates of atomic oxygen must be expressed as a function of the plasma parameters, and the plasma parameters must also be specified as a function of spatial coordinates.

The description of the plasma torus that is adopted for modeling purposes in this paper will be limited to the electrons. Ion-ion and ion-neutral collision processes will be included in future modeling when improved spatial density information for the ion species becomes available. We adopt an electron density-temperature spatial distribution based on Voyager experimental data. A single Maxwellian electron energy distribution is applied although we realize such a description is not strictly correct since it is known that the electrons are non-Maxwellian and that the microscopic state varies with radius and magnetic latitude within the torus (Scudder, Sittler and Bridge, 1981). This non-Maxwellian distribution is actually characterized by a dominant cool component (5-26ev) and a small hot component (626-1200 ev). The relative abundance of the hot component measured at Voyager 1 encounter increases with radius, having values of 0.02%, 1.38% and 7.93% for radial values of 5.5, 7.8 and 8.9 Jupiter radii (R_j) respectively (Scudder, Sittler, and Bridge, 1981). Further, observations of an upper limit of OIII abundance in the hot torus (Brown, Shemansky and Johnson, 1983) have placed a stringent upper limit on the high energy electron component in the

post Voyager 2 encounter epoch. According to the Brown, Shemansky and Johnson calculations, which include charge exchange reactions in the central region of the torus, the limitation on the population of hot electrons is relatively independent of ion diffusive loss time. Quantitatively, a relative hot electron abundance of only 0.02% is above the limit indicated in the latter work. On this basis, the contribution of the hot component to the electron impact ionization and to the 6300 Å, 1304 Å and 880 Å excitations of atomic oxygen is not significant compared to the cool component contribution. Although ionization rate coefficients are much higher for the hot electron component, the density relative to the cool component is too low to contribute significantly to the lifetime (see Table 1). Excitation of 6300 Å emission is inefficient at high temperatures (Table 1) whereas excitation of 1304 Å and 880 Å is higher (Table 1) but is offset by the low density of the hot component. Because of this, specification of only the low temperature electron component of the plasma is required in the modeling work to follow.

Figure 1 shows the two radial temperature profiles that have been adopted in this paper for the cool electrons in the torus appropriate to the two encounter conditions of Voyager 1 and Voyager 2 with Jupiter. The ion temperature profile for the Voyager 1 encounter condition is also indicated for comparison, as deduced from the <u>in situ</u> direct plasma measurements by Bagenal and Sullivan (1981) using their common temperature model. For radial displacements from Jupiter less than 4.9 R_j, the adopted electron temperatures in Figure 1 are assumed to have a constant value of 5.8×10^3 K (0.5 ev), whereas for radial displacements from 4.9 R_j to 5.3 R_j values equal to the measured ion temperature are assumed. For radial distances from 5.3 R_j to 7.0 R_j, the electron temperatures are equal to average electron temperatures

deduced from analysis of the extreme ultraviolet emission from the torus ions obtained by the UVS instrument of the Voyager 1 and Voyager 2 spacecraft. In the 7.0 to 8.5 R_J region, temperatures are interpolated using the *in situ* measurements of Scudder, Sittler and Bridge (1981) for the Voyager 1 epoch, at 7.8 and 8.9 R_J. Scudder, Sittler and Bridge (1981) also provide a measured temperature at 5.5 R_J which lies approximately 20 percent below the interpolated curve in Figure 1. Beyond 8.5 R_j the electron temperatures are assumed to have a constant value of 3×10^5 K (25.8 ev). The exact value of the temperature beyond 8.5 R_j is not important since ionization rates show little dependence in this temperature region. The Voyager 2 epoch curve beyond 7.0 R_J is established by assuming the terminal temperature at 8.5 R_J was the same as the measured value at the Voyager 1 encounter.

The radial profile of the electron number densities in the centrifugal equator of the Io plasma torus, appropriate to the encounter conditions of Voyager 1 and Voyager 2 with Jupiter, is shown in Figure 2. The two electron density profiles from the Voyager 1 *in situ* plasma data (Bridge, Sullivan and Bagenal, 1980; Bagenal and Sullivan, 1981; Bagenal, 1981), deduced by equating them to the magnitude of the total ion charge density for the common temperature and thermal speed models, are shown between the radial distances of 4.0 R_j and 8.5 R_j. The two profiles are identical for radial displacements less than 5.8 R_j, and an extrapolated value has been assumed between 4.0 R_j and 4.9 R_j based upon refined data at 4.9 R_j and 5.0 R_j provided by Bagenal (1981). The average electron number density profiles obtained from analysis of the ultraviolet ion emission data from the plasma torus measured by the UVS instruments of Voyager 1 and Voyager 2 are also indicated and have been enhanced by a multiplicative factor of 1.25. This enhancement factor has been

chosen to adjust the spatially averaged values of the Voyager 1 electron density determined from the UVS data to their maximum values in the centrifugal plane as defined by the Voyager 1 in situ plasma data. For model calculations appropriate to the Voyager 1 encounter conditions, the adopted number densities in the centrifugal plane are defined by the in situ results from 4.0 R_J to 5.8 R_J and by the enhanced UVS results for radial displacements larger than 5.8 R_J. For model calculations appropriate to the Voyager 2 encounter conditions, the adopted number density in the centrifugal plane will be defined by the in situ Voyager 1 results increased by a multiplicative factor of 1.4 in the radial interval from from 4.0 R_j to 5.8 R_j and by the modified UVS results of Voyager 2 for radial displacements larger than 5.8 R_j.

In the model calculations described below, the electron number density in the Io plasma torus is specified in two-dimensions, n(r,z), having radial (r) and vertical (z) dependencies above and below the centrifugal plane. The number density is assumed to be independent of magnetic longitude. The two-dimensional electron number density profiles in the centrifugal plane are determined from the radial number density profiles in the centrifugal equator, n(r) adopted in Figure 2, by an approximate form of a scaling law utilized earlier by Bagenal and Sullivan (1980),

$$n(r,z) = n(r)\, e^{-(z/H)^2}. \qquad (1)$$

In this expression the distance along the magnetic field line from the centrifugal plane has been approximated by the vertical distance from the centrifugal plane. This approximation is acceptable for the small vertical departures of interest in the Io plasma torus. The scale height H, in units of km, is defined by

$$H^2 = (1.7924 \times 10^5)\, \frac{T}{M} \qquad (2)$$

where the temperature T, in units of ^{o}K, has been chosen as the cool component electron temperature profile adopted in Figure 1. The value of the effective Mass M, in units of AMU, has been selected to be 8.2 by requiring the calculated number density n(r,z) for the Voyager 1 encounter conditions to be in reasonably good agreement with the more carefully described two-dimensional electron number density distribution reported by Bagenal and Sullivan (1981).

Having specified the spatial dependence of the electron temperature and number density in the torus, the electron impact ionization lifetime and the 6300 Å, 1304 Å and 880 Å volume excitation rates for atomic oxygen can be determined using the data in Table 2. The excitation rates given in Table 2 were calculated using the Brook, Harrison and Smith (1978) measurements of the OI ionization cross-section and an OI electron excitation model calculated by Shemansky (unpublished) based on available measured and theoretical collision strengths (see Table 2). The 6300 Å collision strengths, in particular, were based upon the Henry, Burke and Sinfailam (1969) calculations. Equivalent analytic expressions were used in the model calculations. The two-dimensional electron-impact ionization lifetime for oxygen in the torus is illustrated in Figure 3 for the Voyager 2 encounter conditions. These conditions are appropriate for the observations of Brown (1981). The motion of Io in the torus caused by the oscillation of the plasma torus about the satellite orbit plane is illustrated and causes a variation of a factor about 6 in the oxygen lifetime at the satellite location. In the present model the centrifugal plane and the satellite orbit plane are assumed coincident so that no oscillation of the plasma is included.

To model the two-dimensional sky-plane intensity map of the 6300 Å, 1304 Å and 880 Å emissions, many atoms are emitted from Io and the lifetime and excitation rates along their orbits are appropriately calculated and spatially tabulated. For model results in this paper, 1298 individual orbits are emitted radially and isotropically from Io's exobase (assumed 2600 km in radius), each with an initial speed of 2.6 km s^{-1}. This value of 2.6 km s^{-1} represents a likely value for the mean speed of an initial velocity dispersion and was chosen because it has been the value best suited for modeling the spatial morphology of the bright Io sodium cloud (Smyth and McElroy, 1978; Smyth, 1979 and 1982). The implicaton of velocity dispersion will be discussed later. Each trajectory in the model is associated with an ensemble of oxygen atoms emitted from a surface element of the satellite exobase. In model calculations, the flight time of atom trajectories must be selected sufficiently long to insure that a steady state description of the neutral gas cloud has been achieved. In all model results to follow, flight times of 500 hours and 1000 hours were suitable for the Voyager 1 and Voyager 2 encounter conditions respectively. The flux of the oxygen atoms emitted from Io is determined by requiring that the calculated and measured 6300 Å intensities are identical.

3. Model Results

The spatial morphologies of the emission intensities, neutral density and ion creaton rate for the Io atomic oxygen cloud have been calculated using the model described in Section 2. Because the only detection of the cloud has been the observation of its 6300 Å intensity (Brown, 1981), model calculations to be presented will emphasize results at this wavelength and only briefly discuss intensity results for the wavelengths of 1304 Å and 880 Å.

Model results for the 6300 Å intensity on the sky plane, appropriate to the detection observation of Brown (1981), are shown in Figure 4 where Voyager 2 plasma encounter conditions have been assumed. The two locations of Brown's observing slit are indicated, centered at 5.0 and 5.9 R_j. His intensity measurement of 8 Rayleighs is an average of six 30 minute exposures, two taken at the 5.0 R_j slit location. This average intensity is achieved by our model calculation for an isotropic satellite escape flux of 1.5×10^9 atoms cm^{-2} s^{-1} or a total source rate of 6.2×10^{26} atoms s^{-1}. The intensity contours in Figure 4, labeled in Rayleighs, are evaluated for this value of the oxygen source. Using the hotter plasma conditions at the time of the encounter of Voyager 1 with Jupiter, the neutral source rate is a factor of two larger, i.e., 1.2×10^{27} atoms s^{-1}.

In Figure 4, the oxygen cloud is seen to completely encircle Jupiter, having a non-uniform intensity peaked near Io and also near the elongation point of the satellite orbit. If Brown had used only one slit location and had centered it more optimally at 5.72 R_j rather than at 5.9 R_j, the model calculation predicts that a signal of 14.8 Rayleighs would have been measured. The spatial variations of the 1304 Å and 880 Å intensities on the sky plane are similar in pattern to those of the 6300 Å intensity in Figure 4. The

absolute intensity of the 1304 Å emission is comparable to the 6300 Å intensity for the Voyager 1 encounter plasma conditions and about two-thirds of this value for the Voyager 2 encounter conditions. The absolute intensity of the 880 Å emission is about a factor of five smaller than the 6300 Å intensity for the Voyager 1 encounter conditions and about a factor of ten smaller for the Voyager 2 encounter conditions. In Table 2, the 6 Rayleigh upper limit of the 1304 Å intensity determined by long-integration-time measurements of the IUE satellite UV instrument exceeds, because of its relatively large viewing aperature, the corresponding model simulated value. The other upper limit for the 1304 Å emission intensity of 25 Rayleighs in Table 2 was established by the Voyager 1 UVS instrument when its much smaller rectangular viewing slit (0.5 R_J x 0.05 R_J) was centered on the satellite. Near Io the model calculated emission brightnesses are approximately symmetric north, south, east and west of the satellite inside a radius of about 0.5 R_J. Model calculated values of the 1304 Å intensity seen by the UV slit are 14 Rayleighs for Voyager 1 encounter conditions and 6 Rayleighs for the Voyager 2 encounter conditions, both below the measured upper limit. The 10 Rayleigh upper limit of 880 Å emission intensity in Table 2 is also well above the model calculated value.

The morphology of the 6300 Å intensity viewed from above the satellite orbit plane and corresponding to the model calculation of Figure 4 is shown in Figure 5. The intensity is brightest near Io and is moderately bright ahead of the satellite and just inside its orbit, where the temperature is still sufficiently hot to excite the line emission and where neutral oxygen is relatively abundant. The distribution of neutral oxygen is shown from the same viewing perspective in Figure 6. Oxygen atoms are seen to be

concentrated primarily inside of the satellite orbit where the electrons are too cold for ionization of the cloud. Charge exchange not included in these model calculations, will, however, modify to some extent the neutral distribution inside of Io's circular orbit. The calculated instantaneous ion creation rate produced by electron impact ionization of the oxygen cloud and corresponding to the results of Figure 6 is presented in Figure 7. Ahead of Io, the ions are mostly created just inside of the satellite orbit, whereas behind Io, most ions are created outside of the satellite orbit and somewhat nearer the satellite where ionization lifetime has its minimum value (see Figure 3). This overall spatial pattern is a direct consequence of the motion of neutrals in the gravitational force fields of Io and Jupiter and the spatial structure of the lifetime of oxygen in the plasma torus.

A radial profile for the abundance of neutral oxygen and for the ion creation rate can be produced by integrating the individual three-dimensional distributions over the angular dimension around Jupiter and the vertical dimension normal to the satellite plane. These radially averaged profiles, so constructed for radial integration-intervals of 0.1 Jupiter radii, are presented in Figure 8. The profiles were computed for the same Voyager 2 plasma conditions and satellite emission conditions assumed in Figures 4-7. The oxygen cloud contains 2.28×10^{32} atoms and the total ion source rate of 6.20×10^{26} ions s^{-1}. The abundance of neutrals is seen to decrease rapidly outside of Io's orbit while the ion creation rate is somewhat inflated because of the minimum lifetime of oxygen at 7.3 R_j (see Figure 3). Inside of Io's orbit the neutrals are more abundant and the ion creation rate drops rapidly because of the precipitous decrease in the electron temperature (see Figures 1 and 3).

4. Implications for the Plasma Torus

The calculations presented in Section 3 for the atomic oxygen cloud are a necessary first step in better understanding several physical processes that take place in the Io plasma torus. The rate at which oxygen atoms are lost by the neutral cloud may be directly used to provide a lower limit for the ion loading rate $\dot{N}$, plasma mass loading rate $\dot{M}$ and ion energy input rate $\dot{E}$ to the plasma torus. The oxygen results determine only lower limits for these three quantities since other yet unidentified direct plasma sources may also exist for the magnetosphere as well as other neutral gas clouds. The lower limit for the ion loading rate $\dot{N}$ may then be used to estimate an upper limit for the ion residence time (i.e., an ion-diffusion loss time) in the plasma torus and thereby constrain the form of the plasma diffusion coefficient for the magnetosphere.

The procedure to be utilized here for atomic oxygen may be generalized to several neutral gas clouds (O, S, etc.) where charge exchange is included and requires that only the neutral loss rates L_j and the neutral production rates P_j be calculated for each of the neutral species j. In the general case

$$\dot{N} = -\sum_j (P_j - L_j) \qquad (3)$$

$$\dot{M} = -\sum_j m_j (P_j - L_j) \qquad (4)$$

$$\dot{E} = -\sum_j 1/2\ m_j \left[V_T^2\ P_j - V_R^2\ L_j\right] \qquad (5)$$

where m_j is the mass of the j^{th} neutral species, V_T is the average thermal velocity of an ion previous to being converted to the j^{th} neutral species (which then escapes the Jupiter system), and V_R is the relative velocity of an ion with respect to the rotating magnetosphere upon being produced by

ionization of the j^{th} neutral species. The expression for $\dot{N}$ and $\dot{M}$ follow directly from conservation requirements between the ion, electron, and neutral components, and the expression for E assumes that ion-ion charge exchange reactions do not significantly provide a net production or loss of plasma torus energy. In contrast to the plasma mass loading rate (4), a mass loss rate for the neutral cloud $\dot{M}_c$ may also be defined:

$$\dot{M}_c = \sum_j m_j L_j \qquad (6)$$

The results of Section 3 represent the simplest case for the quantities (3) - (6), where the neutral loss rate depends only upon electron impact ionization of atomic oxygen and where the neutral production rate is zero:

$$\dot{N} = L_o \qquad (7)$$

$$\dot{M} = \dot{M}_c = m_o L_o \qquad (8)$$

$$\dot{E} = 1/2\ m_o V_R^2 L_o \qquad (9)$$

The radial profile for L_o calculated for the plasma encounter conditions of Voyager 2 is given in Figure 8 by the oxygen ion creation rate and produces spatially integrated source rates for $\dot{N}$, $\dot{M}$, and $\dot{E}$ of 6.2×10^{26} ions s^{-1}, 16.6 kg s^{-1}, and 2.7×10^{10} watts respectively. In calculating this last quantity, a value of 56.8 km s^{-1} for V_R was assumed and determined by the relative motion of Io and the rotating magnetosphere. An upper limit for the ion-diffusive loss time τ in the plasma torus may be estimated from $\dot{N}$ as follows

$$\tau = \left(\frac{\dot{N}}{N}\right)^{-1} \qquad (10)$$

where N is the number of ions in the spatial element in which $\dot{N}$ is calculated. Using the spatially integrated source rate $\int \dot{N}$, and an estimated total of 2.7×10^{34} ions, the averaged ion-diffusive loss time is constrained to 500 days. This relatively large value is reduced significantly when additional contributions to $\dot{N}$, roughly estimated below, are included for a sulfur gas cloud and for charge exchange processes. The spatially integrated value of 2.7×10^{10} watts for $\dot{E}$, which represents less than 1% of the 3×10^{12} watts radiated by the UV torus, will likewise be significantly increased by these additional contributions estimated below. For the plasma encounter conditions of Voyager 1, the spatially integrated source rates for $\dot{N}$, $\dot{M}$, and $\dot{E}$ are a factor of two larger than those given above, if it is assumed the 6300 Å intensity at this earlier time had the same brightness.

The strength of the conclusions drawn above from the results of Section 3 are limited to some extent by several uncertainties in modeling. Inaccuracies in excitation cross-sections as well as in data that specify the plasma torus properties could produce changes to increase or decrease the results. The lack of knowledge about the oxygen source characteristics of Io (i.e., the importance of higher velocity components in the dispersion of the emission velocity distribution and its exospheric distribution) could raise the overall satellite flux required to maintain the observed 6300 Å brightness, but competing processes make the overall effect difficult to estimate without further observational information about the angular extent of the atomic oxygen cloud. On the other hand, inclusion of an oscillating torus in the model would produce a longer average lifetime for atomic oxygen and would therfore likely reduce the satellite flux required to match a given 6300 Å observation. The two oppositely directed effects may to first order cancel each other.

Significant modifications of the conclusions drawn above from the results of Section 3 may, however, be anticipated from two factors not included in the model: (1) the likely existence of a neutral sulfur cloud for Io and (2) the importance of several neutral-ion and ion-ion charge exchange reactions in the plasma torus involving the species OI, OII, OIII, OIV, SI, SII, SIII, and SIV. The presence of charge exchange reactions involving slow neutrals and fast corotating ions of the form

$$\text{neutral} + \text{ion} \rightarrow \text{ion} + \text{neutral} \qquad (11)$$

$$\text{neutral} + \text{ion} \rightarrow \text{ion} + \text{ion} \qquad (12)$$

both enhance and couple the oxygen and sulfur loss rates as well as provide substantial neutral production rates. An improved model incorporating this coupling is then required to accurately describe the neutral clouds and their impact on the magnetosphere. Lacking this coupling in the present model and the necessary information about the presence of neutral sulfur in the Jovian environment, this impact may be roughly estimated by scaling the above spatially integrated model results by the model calculation of Brown, Shemansky and Johnson (1983). In their calculation, the ratio of the overall oxygen to sulfur loss rate was assumed to be two, which is the ratio for a satellite loss rate based upon the source molecule SO_2. Using this calculation as a guide, the spatially integrated value of the oxygen loss rate L_O calculated above for electron impact ionization only is enhanced by a factor of eight by charge exchange reactions, providing a scaled value of 5×10^{27} OI atoms s^{-1}. The spatially integrated values of the sulfur loss rate L_S is then one-half this value or 2.5×10^{27} SI atoms s^{-1}. These two

loss rates are equivalent to satellite fluxes of 1.2×10^{10} OI atoms $cm^{-2}s^{-1}$ and 6.0×10^{9} SI atoms $cm^{-2}\ s^{-1}$ respectively. The spatially integrated values of the oxygen production rate P_o and sulfur production rate P_s may likewise be scaled using the results of Brown, Shemansky and Johnson (1983) by a factor of approximately 0.6 and 0.3 times their respective loss rates yielding values of 3.0×10^{27} OI atoms s^{-1} and 0.75×10^{27} SI atoms s^{-1}. These production rates arise from the charge exchange reactions (11) and also from electron recombination reactions.

Using these approximations for the production and loss rates for neutral oxygen and sulfur in the expressions (3) through (6), more realistic values for the ion loading rate, the plasma mass loading rate, the cloud mass loss rate, and the ion energy input rate for the plasma torus may be calculated and expressed as

$$\dot{N} = 0.75(L_o) \tag{13}$$

$$\dot{M} = 1.1(m_o L_o) \tag{14}$$

$$\dot{M}_c = 2.0(m_o L_o) \tag{15}$$

$$\dot{E} = 2.0(1/2\ m_o V_R^2)L_o - 0.9(1/2\ m_o V_T^2)L_o \tag{16}$$

where the spatially integrated value of L_o is 5×10^{27} ions s^{-1}. The effects of charge exchange have thus been to modify the simple dependence exhibited between $\dot{N}$, $\dot{M}$, $\dot{M}_c$ and $\dot{E}$ in the earlier derived expressions (7), (8) and (9) which were based only on electron impact inonization. The spatially integrated value of the ion loading rate (13) is then 3.85×10^{27} ions s^{-1} and implies a value for the ion diffusive loss time (10) of 200 days, assuming a density of 1380 cm^{-3} (appropriate to the Voyager 2 encounter) and a plasma

torus of $1R_J$ radius centered on Io's orbit. The spatially integrated value of the plasma mass loading rate (14) is 146 kg s^{-1} of which 53 kg s^{-1} is supplied by oxygen atoms and 93 kg s^{-1} by sulfur atoms. In contrast, the spatially integrated value for the mass loss rate of the neutral cloud (15) is 266 kg s^{-1}. The spatially integrated value of the ion energy input (16) is 3.9×10^{11} watts, using a value for V_T = 26.9 km/s appropriate to the average temperature of 60 eV reported by Brown (1982) for S^+, or is 4.3×10^{11} watts using a smaller thermal speed for the ions of 7.6 km s^{-1}. These two values of the ion energy input rate represent respectively 13% and 14% of the 3×10^{12} watts radiated by the plasma torus in UV wavelengths. This ion energy input is similar in magnitude to the Io correlated energy source discovered by Sandel and Broadfoot (1982) which supplies about 20% of the UV radiated power.

To determine the spatial variations of the ion number, mass and energy injection rates in the plasma torus supplied by the neutral clouds, more refined model calculations (which are currently under development) will be required. The overall spatial character of these processes for oxygen or sulfur may however be understood as being controlled through three channels if charge exchange reactions are considered. Electron ionization in the present model would tend to dominate in radial regions more distant than 6.7 R_J. In the radial interval 5.6 to 6.7 R_J, roughly equal contributions from electron impact ionization and charge exchange are expected. Charge exchange reactions will dominate inside of 5.6 R_J where the electron temperature decreases rapidly. Charge exchange processes are therefore expected to modify the radial distribution of OI atoms and the ion creation rate shown in Figure 8 which are calculated only for electron impact ionization. For radial

displacements larger than 5.9 R_J, the rather sharp reduction in the OI population and the substantial ion creation rate out to 7.5 R_J are caused by the rapidly rising elecron ionization rate coefficient and these features will have the same character when charge exchange is included. The drop in the ion creation rate through two decades in the inward direction from 5.9 R_J to 5.5 R_J occurs because of the precipitous drop in the electron temperature in that region. The inclusion of charge exchange reactions will provide a new ion production mechanism inward of 5.9 R_J which will enhance the ion creation rate and will also sharpen the neutral atom distribution by reducing the relative number of atoms in the 4.5 to 5.5 R_J region. The extent of the oxygen cloud will also be confined more closely to the position of Io and the radial distribution of oxygen may then tend to show a slightly higher density peak than that shown in Figure 8, because the Brown (1981) observation was made ~90° downstream from the position of Io.

The above estimates for the ion loading rate, the mass loading rate and the ion energy loading rate for the plasma torus have as their source the neutral gas clouds of Io. Although it is almost certain that Io is the ultimate source of these ions, other sources of neutrals or direct sources of ions that have yet to be discovered might also exist in addition to the ions created by the neutral gas clouds. If the other sources of ions are significant, the above estimates of $\dot{N}$, $\dot{M}$ and $\dot{E}$ are only lower limits. It is difficult to assess the possible magnitude of direct ion sources since knowledge of Io's atmosphere and the mechanisms which deliver the material to the torus is very limited. Only oxygen ionization processes that occur in the near vicinity of Io have been limited by direct observation and predictable emission efficiencies (Shemansky 1980). The Shemansky (1980) upper limit on

direct ion injection from Io is roughly 10^{27} s^{-1} based on ion detection of the OI 1304 Å line in Voyger 1 observations. Attempts to observe the 1304 Å line by Moos and Clarke (1981) using the IUE satellite produce about the same value, 10^{27} s^{-1}, as an upper limit for the Voyager 1 encounter epoch. It is likely that the source molecule supplying the neutral gas clouds is SO_2 (Pearl et al., 1979; Johnson et al., 1979) so that direct escape of SO_2, SO_2^+ or its chemical fragments (SO, O_2, etc.) may occur and not have as yet been detected. The assessment of the importance of these molecules and ions as a source of plasma for the magnetosphere will, however, require that additional information be acquired.

5. Concluding Remarks

A model has been presented for the neutral oxygen cloud of Io based upon atom-electron impact excitation and ionization processes in the plasma torus. The flux of oxygen atoms emitted from Io was determined by requiring that the measured (Brown 1981) and the calculated 6300 Å intensities be identical. By this means satellite emission fluxes of 3.0×10^9 cm^{-2} s^{-1} and 1.5×10^9 cm^{-2} s^{-1} were required for plasma conditions appropriate to the time of encounter of Voyager 1 and Voyager 2 with Jupiter. The 6300 Å observations of Brown (1981) were more appropriate to the Voyager 2 plasma conditions for which spatially integrated ion loading rates, plasma mass loading rates and ion energy input rates were calculated to be 6.2×10^{26} ions s^{-1}, 16.6 kg s^{-1}, and 2.7×10^{10} watts respectively. This value of the ion loading rate implies an ion-diffusive loss time of 500 days.

Enhanced values of the satellite emission flux, ion loading rate, mass loading rate and ion energy input rate resulting from the presence of a likely existing sulfur cloud and from the impact of charge exchange reactions were then roughly estimated based on the results of the oxygen model and the charge exchange calculations of Brown, Shemansky and Johnson (1983). The upward adjusted value of the satellite flux for atomic oxygen was 1.2×10^{10} cm^{-2} s^{-1} and an additional satellite flux of 6.0×10^9 cm^{-2} s^{-1} was assumed for the likely existing sulfur cloud of Io. This represents a neutral mass loss for the satellite of ~270 kg s^{-1}. The corresponding adjusted values for the spatially integrated ion loading rate, plasma mass loading rate, and ion energy input rate were then 3.8×10^{27} ions s^{-1}, ~150 kg s^{-1} and $(3.9 - 4.3) \times 10^{11}$ watts respectively. This value for the ion loading rate implies an ion-diffusive loss time of ~200 days. The value of the ion energy

input rate represents about 13 - 14% of the 3 x 10^{12} watts radiated in the UV by the plasma torus and is comparable to the 20% energy input level associated with the Io correlated energy source discovered by Sandel and Broadfoot (1982). The remaining 80% of the energy input has been associated by Shemansky and Sandel (1982) with a local time asymmetry in the electron temperature.

Inclusion of charge exchange reactions in future models of the atomic oxygen cloud is important both in refining the values of physical quantities roughly estimated above and in providing an interpretative base for new observations of the neutral and ion species of the magnetosphere. Such a model is presently under development. New observations of the angular distribution of atomic oxygen around Jupiter would be particularly useful in refining the value of the oxygen flux emitted by Io. Observations to detect an atomic sulfur cloud are likewise desirable in order to establish a satellite emission flux for sulfur and thereby better understand processes in the local atmosphere of Io.

Acknowledgements

The contributions of W.H. Smyth and D.E. Shemansky were supported by the NASA Earth and Planetary Exploration Division, Planetary Atmospheres discipline, grants NASW-3503 and NAGW-106, respectively. We wish to thank D.M. Hunten for an editorial reading of the paper. W.H. Smyth wishes to thank M.R. Combi for contributions to the program and for helpful discussion.

Table 1

Observational Data for the Io Atomic Oxygen Cloud

Type of Observation	Investigator	Emission Wavelength (Å)	Brightness (Rayleighs)
1. Ground based	Brown (1981)	6300	8 ± 4
2. IUE Satellite	Moos and Clarke (1981)	1304	<6
3. Voyager UVS	D.E. Shemansky	1304	<25
		880	<10

Table 2

Electron Impact Ionization Rate and Electron Impact Excitation Rates at 6300 Å, 1304 Å and 880 Å for Atomic Oxygen

Electron Temperature (eV)	Ionization Rate[a] ($cm^3 sec^{-1}$)	6300 Å Excitation Rate[b] ($cm^3 sec^{-1}$)	1304 Å Excitation Rate[b] ($cm^3 sec^{-1}$)	880 Å Excitation Rate[b] ($cm^3 sec^{-1}$)
0.5	6.80×10^{-21}	3.44×10^{-11}	1.99×10^{-17}	6.23×10^{-22}
1.0	7.86×10^{-15}	3.20×10^{-10}	3.61×10^{-13}	1.15×10^{-15}
2.0	1.02×10^{-11}	1.09×10^{-9}	5.50×10^{-11}	1.79×10^{-12}
5.0	1.10×10^{-9}	2.40×10^{-9}	1.27×10^{-9}	1.71×10^{-10}
10.0	7.18×10^{-9}	2.92×10^{-9}	3.01×10^{-9}	8.45×10^{-10}
20.0	2.21×10^{-8}	2.72×10^{-9}	6.68×10^{-9}	1.94×10^{-9}
50.0	4.93×10^{-8}	1.70×10^{-9}	9.04×10^{-9}	3.15×10^{-9}
100.0	6.63×10^{-8}	9.25×10^{-10}	9.45×10^{-9}	3.55×10^{-9}
200.0	7.54×10^{-8}	4.25×10^{-10}	9.00×10^{-9}	3.55×10^{-9}
500.0	7.59×10^{-8}	1.28×10^{-10}	7.70×10^{-9}	3.16×10^{-9}
1000.0	7.03×10^{-8}	4.84×10^{-11}	6.54×10^{-9}	2.74×10^{-9}
2000.0	6.19×10^{-8}	1.77×10^{-11}	5.40×10^{-9}	2.29×10^{-9}
5000.0	4.97×10^{-8}	4.56×10^{-12}	4.07×10^{-9}	1.75×10^{-9}

a. Based on ionization cross-section of Brook, Harrison and Smith (1978).

b. Based on OI + e calculations by Shemansky (unpublished); collision strength data for 6300 Å emission were obtained from calculations of Henry, Burke and Sinfailam (1969), measurements by Stone and Zipf (1974) (see Shemansky (1980) for scaling factor) for 1304 Å, and theoretical estimates for 880 Å.

Bagenal, F., 1981, Private Communication

Bagenal, F. and Sullivan, J.D., 1980, Geophys. Res. Lett., 7, 41.

Bagenal, F. and Sullivan, J.D., 1981, J. Geophys. Res., 86, 8447.

Bridge, H.S., Sullivan, J.D., and Bagenal, F., 1980, private communication.

Brook, E., Harrison, M.F.A., and Smith, A.C.H., 1978, J. Phys. B., 11, 3115.

Brown, R.A., 1974, Exploration of the Planetary System, eds. A. Woszczyk and C. Iwaniszewsky, pp. 527-531. Dordrecht, Holland: D. Reidel Pub. Co.

Brown, R.A., 1981, Ap. J., 244, 1072.

Brown, R.A., 1982, J. Geophys. Res., 87, 230.

Brown, R.A. and Shemansky, D.E., 1982, Ap. J., 263, 433.

Brown, R.A., Shemansky, D.E. and Johnson, R.E., 1983, Ap. J., Jan. issue.

Dessler, A.J., 1980, Icarus, 44, 291.

Durrance, S.T., Feldman, P.D. and Weaver, H.A., 1982, EOS, 63, 369.

Eviatar, A. and Siscoe, G.L., 1980, Geophys. Res. Lett., 7, 1085.

Henry, R.J.W., Burke, P.G. and Sinfailam, A.L., 1969, Phys. Rev., 178, 218.

Hill, T.W., 1980, Science, 207, 301.

Johnson, R.E. and Strobel, D.F., 1982, J. Geophys. Res., submitted.

Johnson, T.V., Cook, A.F., Sagan, C., and Soderblom, L.A., 1979, Nature, 280, 246.

Moos, H.W. and Clarke, J.T., 1981, Ap. J., 247, 354.

Munch, G., Trauger, J., and Roesler, F., 1976, Bull. A.A.S., 8, 467.

Pearl, J. et al., 1979, Nature, 280, 755.

Richardson, J.D., Siscoe, G.L., Bagenal, F. and Sullivan, J.D., 1980, Geophys. Res. Lett., 7, 37.

Richardson, J.D. and Siscoe, G.L., 1981, J. Geophys. Res., 86, 8485.

Sandel, B.R. and Broadfoot, A.L., 1982, J. Geophys. Res., 87, 212.

Scudder, J.D., Sittler, E.C., Jr. and Bridge, H.S., 1981, J. Geophys. Res., 86, 8157.

Shemansky, D.E., 1980, Ap. J., 242, 1266.

Shemansky, D.E. and Sandel, B.R., 1982, J. Geophys. Res., 87, 219.

Smyth, W.H., 1979, Ap. J., 234, 1148.

Smyth, W.H., 1982, Ap. J., Oct. issue.

Smyth, W.H. and McElroy, M.B., 1977, Planet. Space Sci., 25, 415.

Smyth, W.H. and McElroy, M.B., 1978, Ap. J., 226, 336.

Stone, E.J. and Zipf, E.C., 1974, J. Chem. Phys., 60, 4237.

Sullivan, J.D. and Siscoe, G.L., 1981, "Satellites of Jupiter," ed. D. Morrison, University of Arizona Press, Tucson.

Thorne, R.M., 1981, Geophys. Res. Lett., 8, 509.

Trafton, L., 1975, Nature, 258, 690.

Trauger, J., Roesler, F. and Munch, G., 1976, Bull. A.A.S., 8, 468.

Figure Captions

Figure 1. Electron Temperature Radial Profiles for the Io Plasma Torus. The two electron temperature profiles adopted for model calculations are discussed in the text. The plotted points are *in situ* measurements from Scudder, Sittler and Bridge (1981).

Figure 2. Electron Number Density Profiles for the Io Plasma Torus. The different number density profiles in the centrifugal plane of the plasma torus are discussed in the text. The two profiles adopted for model calculations are indicated by dashed lines for radial displacements less than 5.8 R_j and by solid lines for larger radial displacements.

Figure 3. Electron Impact Ionization Lifetime (hours) for Atomic Oxygen in the Io Plasma Torus. The lifetime is calculated using the plasma conditions adopted for the Voyager 2 encounter with Jupiter. Ionization cross-sections are based upon the experimental measurements of Brook, Harrison and Smith (1978).

Figure 4. Io Oxygen Torus 6300 Å Emission Intensity. The satellite location and the calculated intensity contours are appropriate to the detection observation of Brown (1981). Voyager 2 encounter plasma conditions and a satellite flux of 1.5×10^9 oxygen atoms cm^{-2} s^{-1} were assumed. See text for discussion.

Figure 5. 6300 Å Oxygen Emission Intensity. The intensity morphology of the Io oxygen cloud viewed from above the satellite orbit plane is calculated for the same plasma and satellite emission conditions of Figure 4. The intensity contours have values, in units of Rayleighs from the outer to inner contour, of 0.045, 0.32, 0.59 and 1.13 respectively.

Figure 6. Io Atomic Oxygen Torus. The column density morphology viewed from above the satellite orbit plane is calculated for the same plasma and satellite emission conditions of Figure 4. The column density contours have values, in units of cm^2 from the outer to the inner contour of 6.6×10^9, 6.7×10^{10}, 1.3×10^{11}, 1.9×10^{11} and 3.1×10^{11} respectively.

Figure 7. Io Oxygen Ion Creation Rate. The ion creation rate morphology viewed from above the satellite orbit plane is calculated for the same plasma and satellite emission conditions of Figure 4. The ion creation rate contours have values, in units of ions cm^{-2} s^{-1} from the outer to the inner contour, of 2.8×10^4, 2.0×10^5, 5.3×10^5, 8.6×10^5 and 1.4×10^6 respectively.

Figure 8. Radial Profiles for Oxygen Abundance and Ion Creation Rate. The profiles are calculated for the same plasma and satellite emission conditions of Figure 4. See text for discussion.

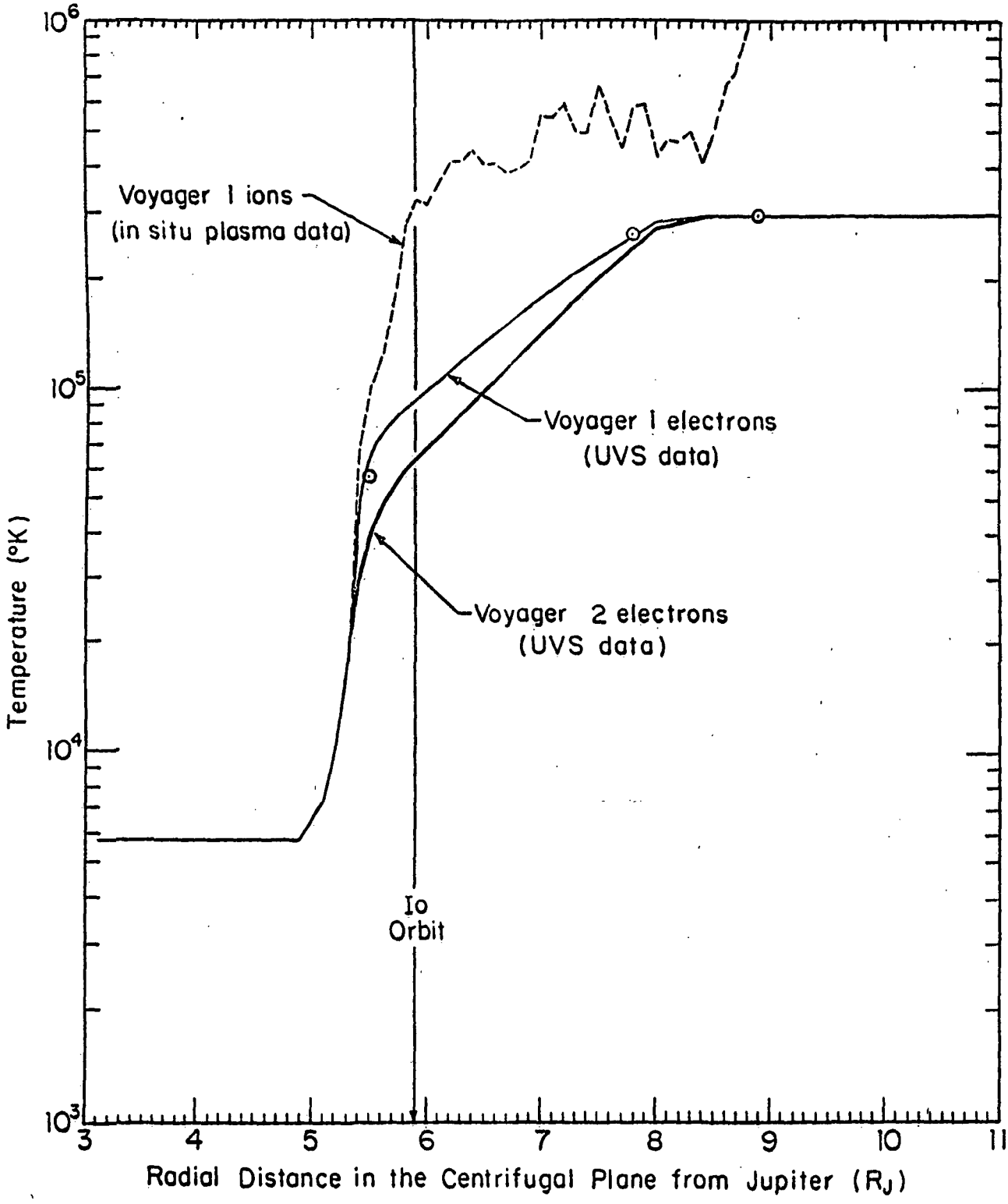
10^6
10^5
10^4
10^3
Temperature (°K)
Voyager 1 ions
(in situ plasma data)
Voyager 1 electrons
(UVS data)
Voyager 2 electrons
(UVS data)
Io
Orbit
3
4
5
6
7
8
9
10
11
Radial Distance in the Centrifugal Plane from Jupiter (R_J)

Figure 1

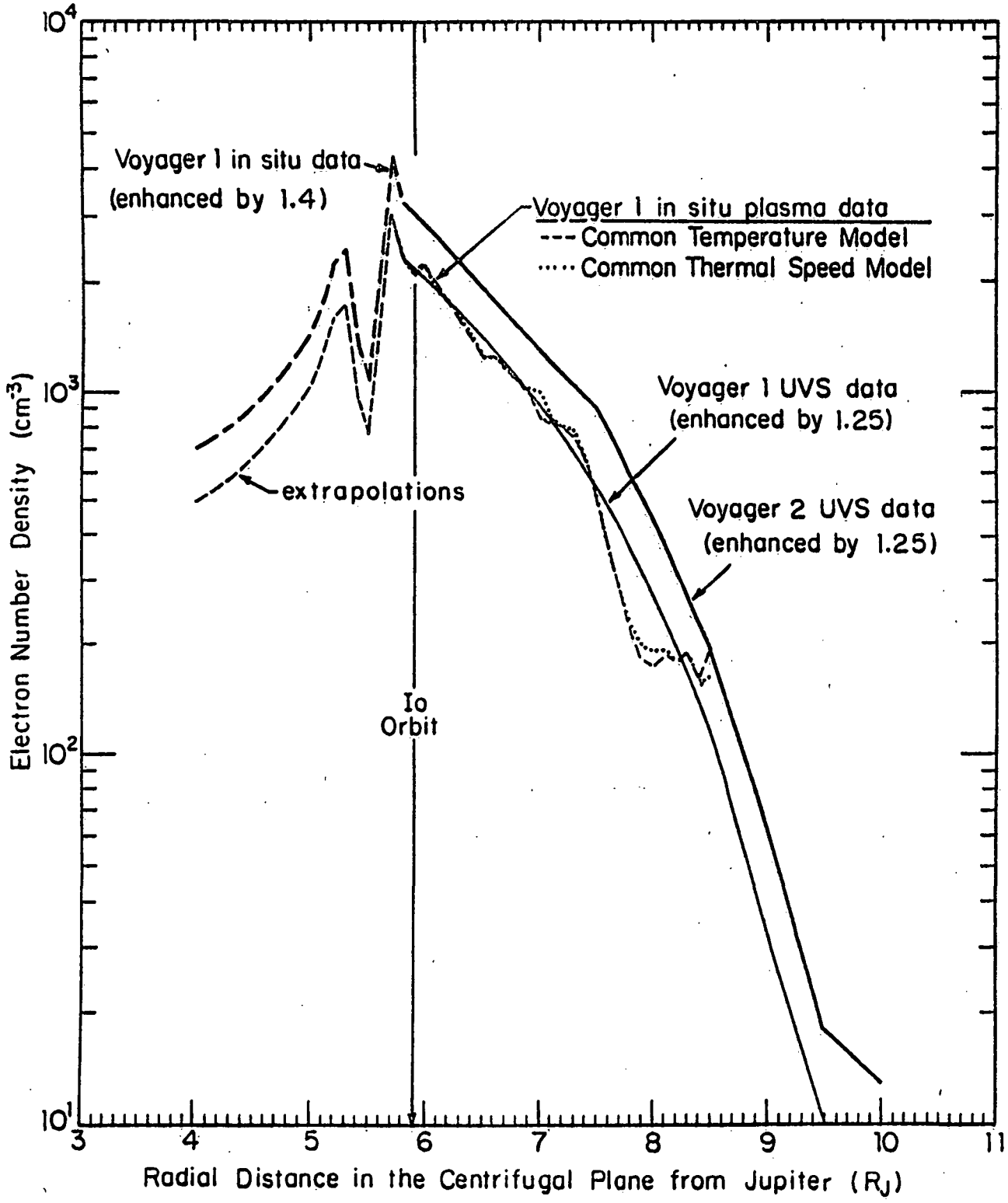
Voyager 1 in situ data
(enhanced by 1.4)
Voyager 1 in situ plasma data
--- Common Temperature Model
····· Common Thermal Speed Model
Voyager 1 UVS data
(enhanced by 1.25)
Voyager 2 UVS data
(enhanced by 1.25)
extrapolations
Io
Orbit
Electron Number Density (cm⁻³)
Radial Distance in the Centrifugal Plane from Jupiter (RJ)

Figure 2

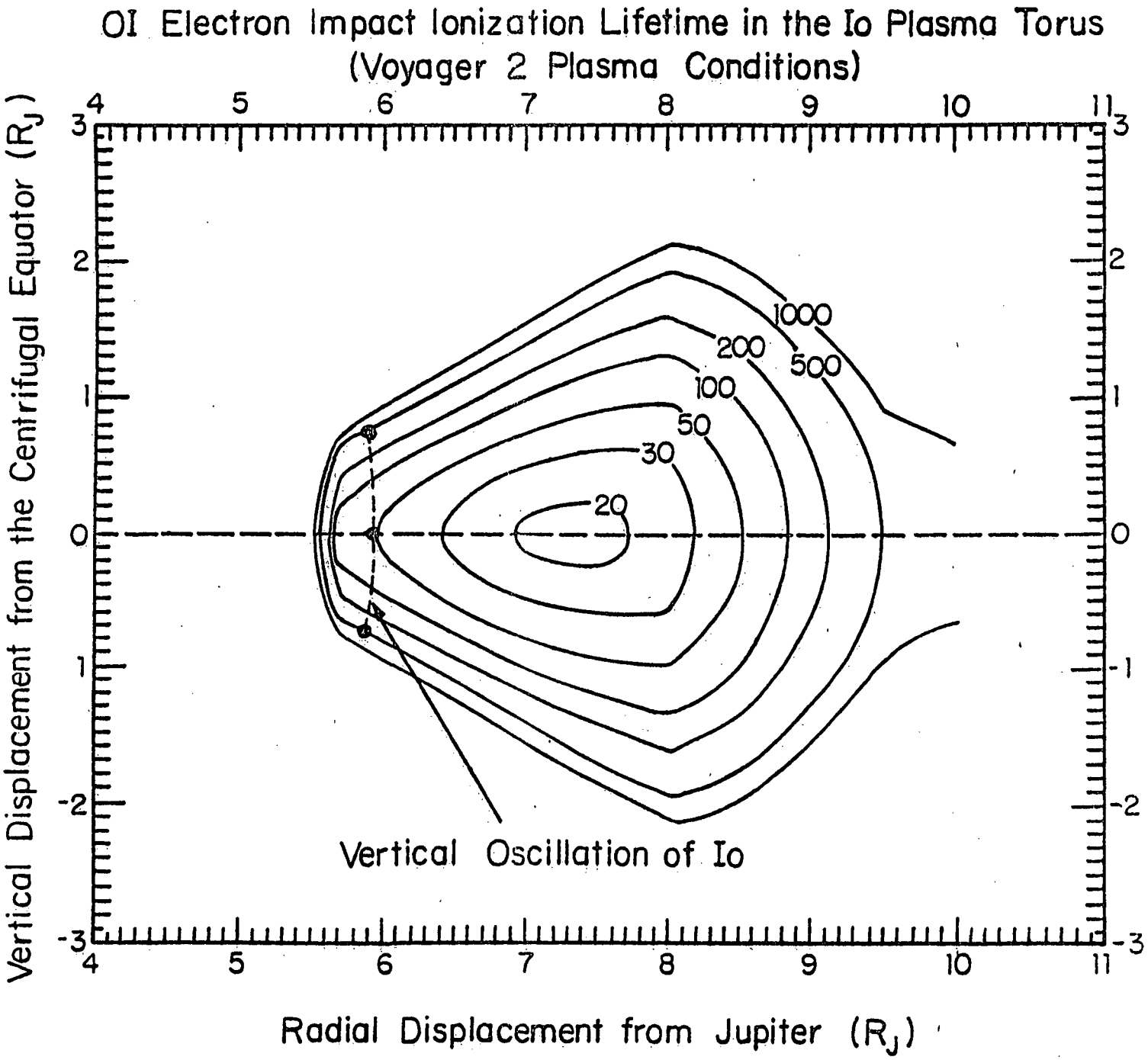
OI Electron Impact Ionization Lifetime in the Io Plasma Torus
(Voyager 2 Plasma Conditions)
Vertical Displacement from the Centrifugal Equator (R_J)
Radial Displacement from Jupiter (R_J)
1000
500
200
100
50
30
20
Vertical Oscillation of Io

Figure 3

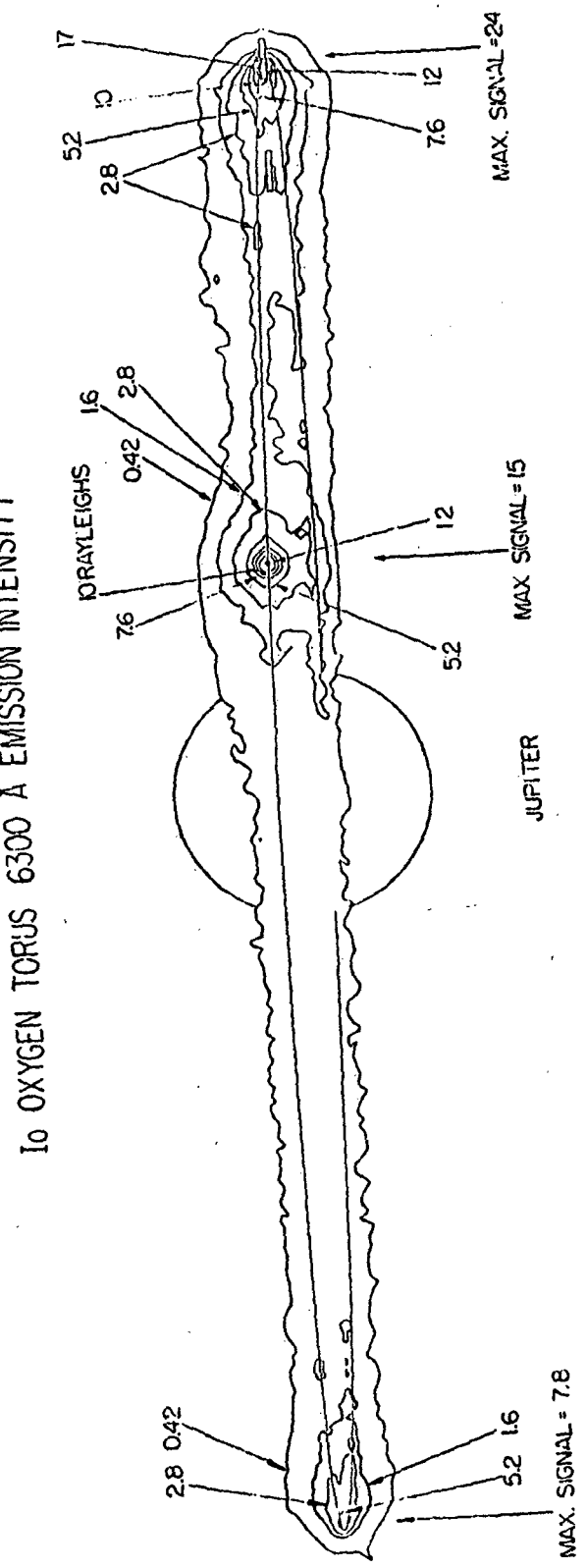
Io OXYGEN TORUS 6300 Å EMISSION INTENSITY
17
10
5.2
2.8
12
7.6
MAX. SIGNAL=24
1.6
2.8
0.42
KRAYLEIGHS
12
MAX SIGNAL=15
7.6
5.2
JUPITER
2.8 0.42
5.2 1.6
MAX. SIGNAL = 7.8

Figure 4

Io: 6300Å Oxygen Emission

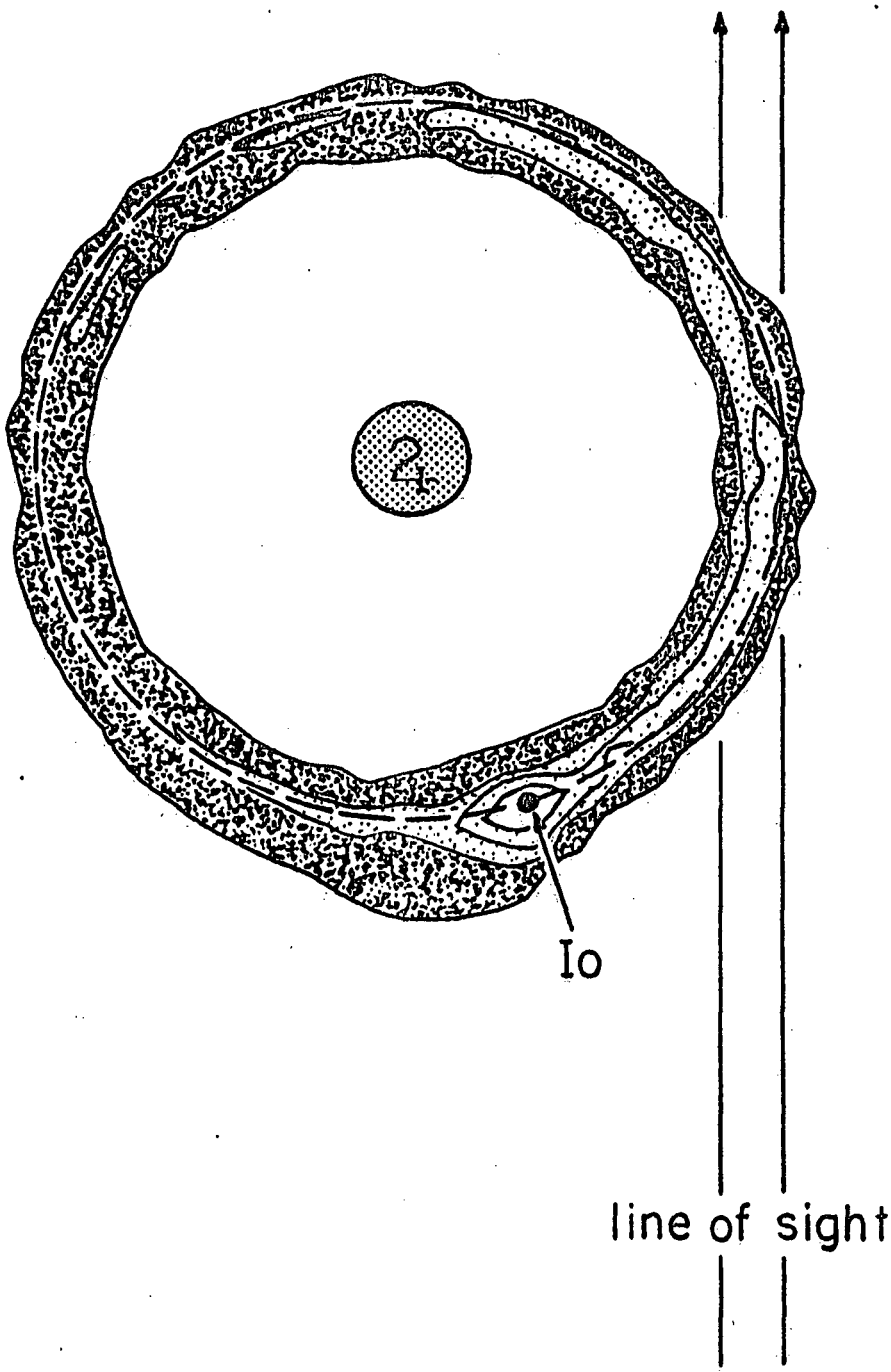

Figure 5

Io: Atomic Oxygen Torus

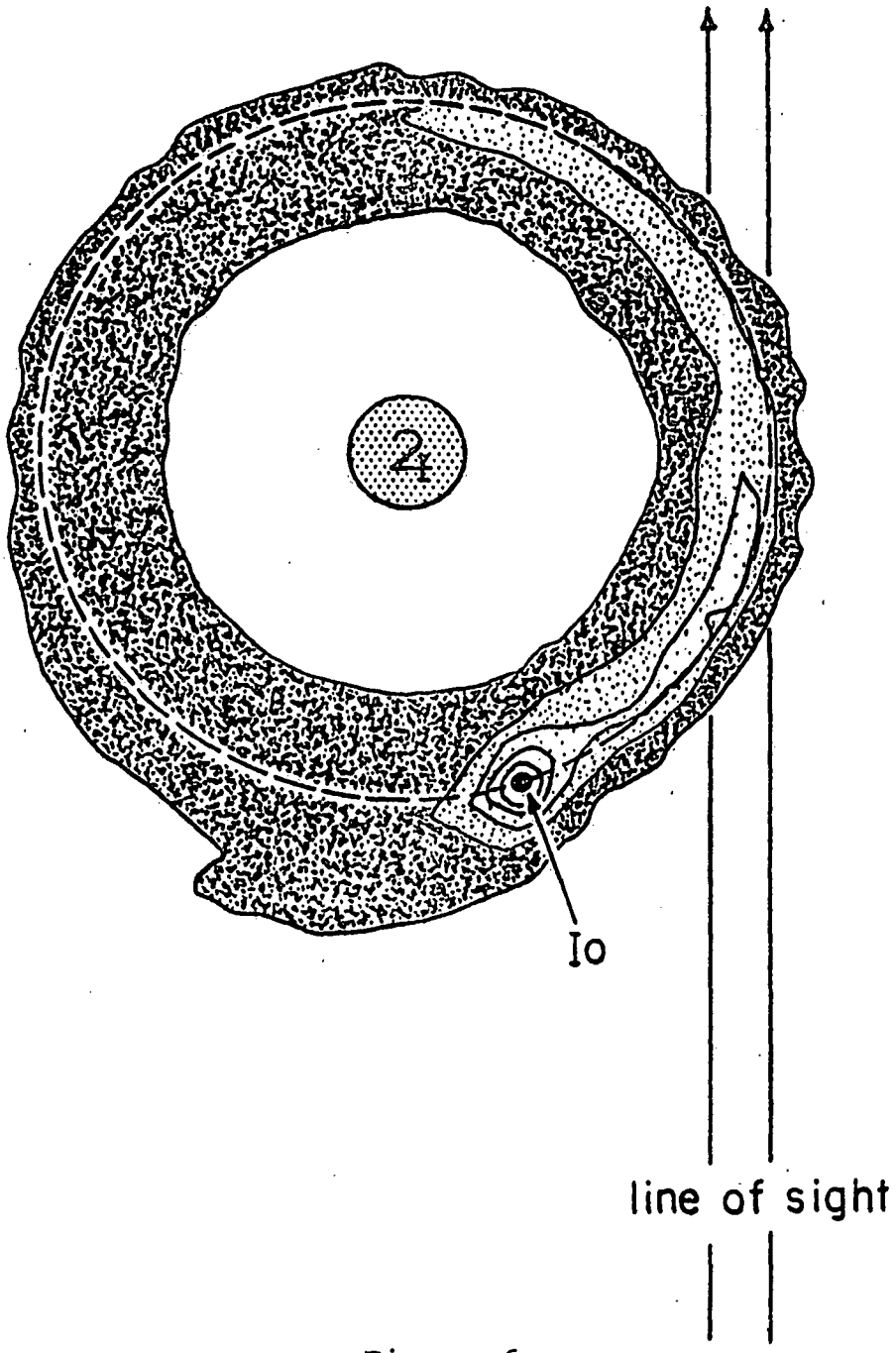

Figure 6

Io: Oxygen Ion Creation Rate

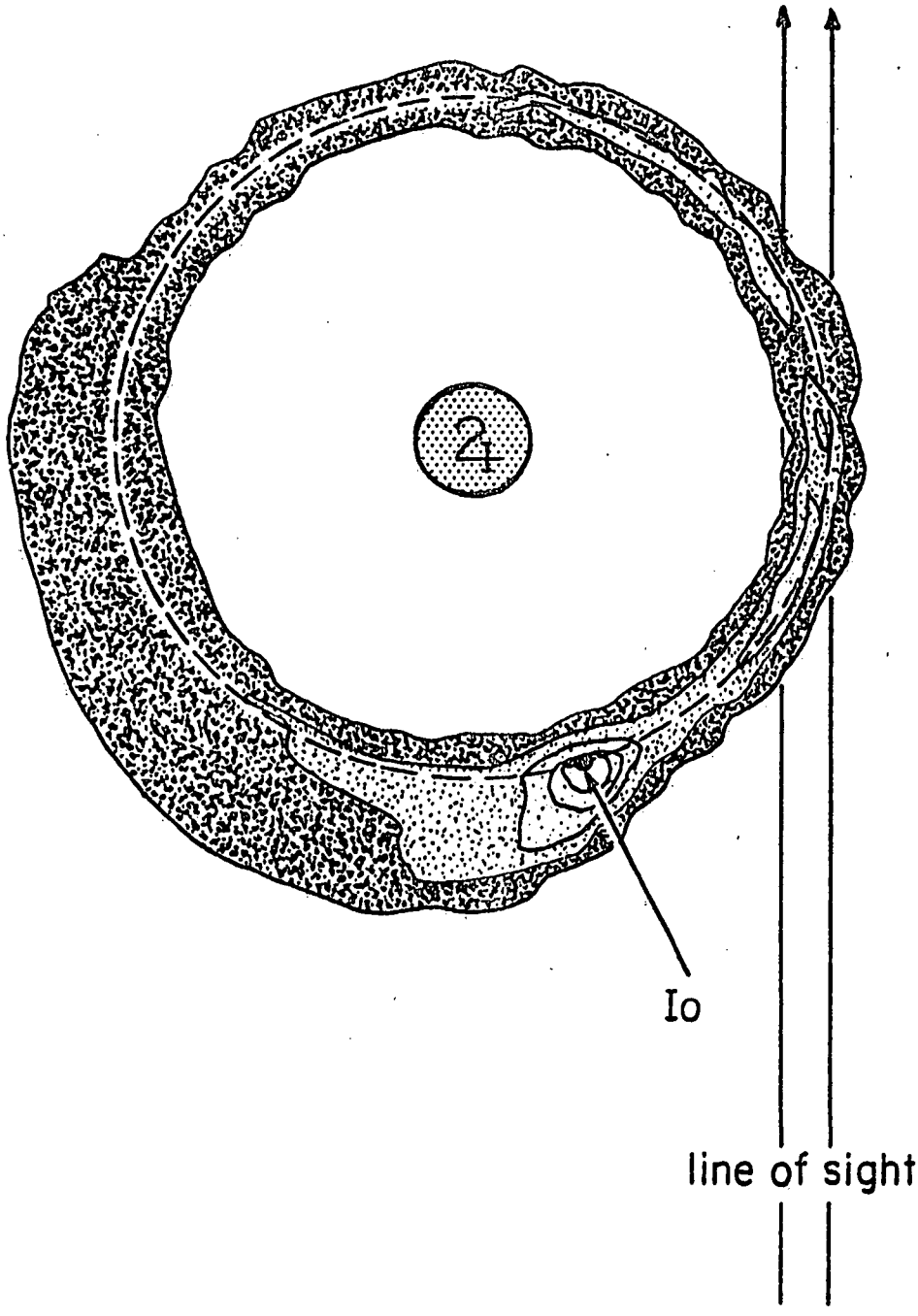

Figure 7

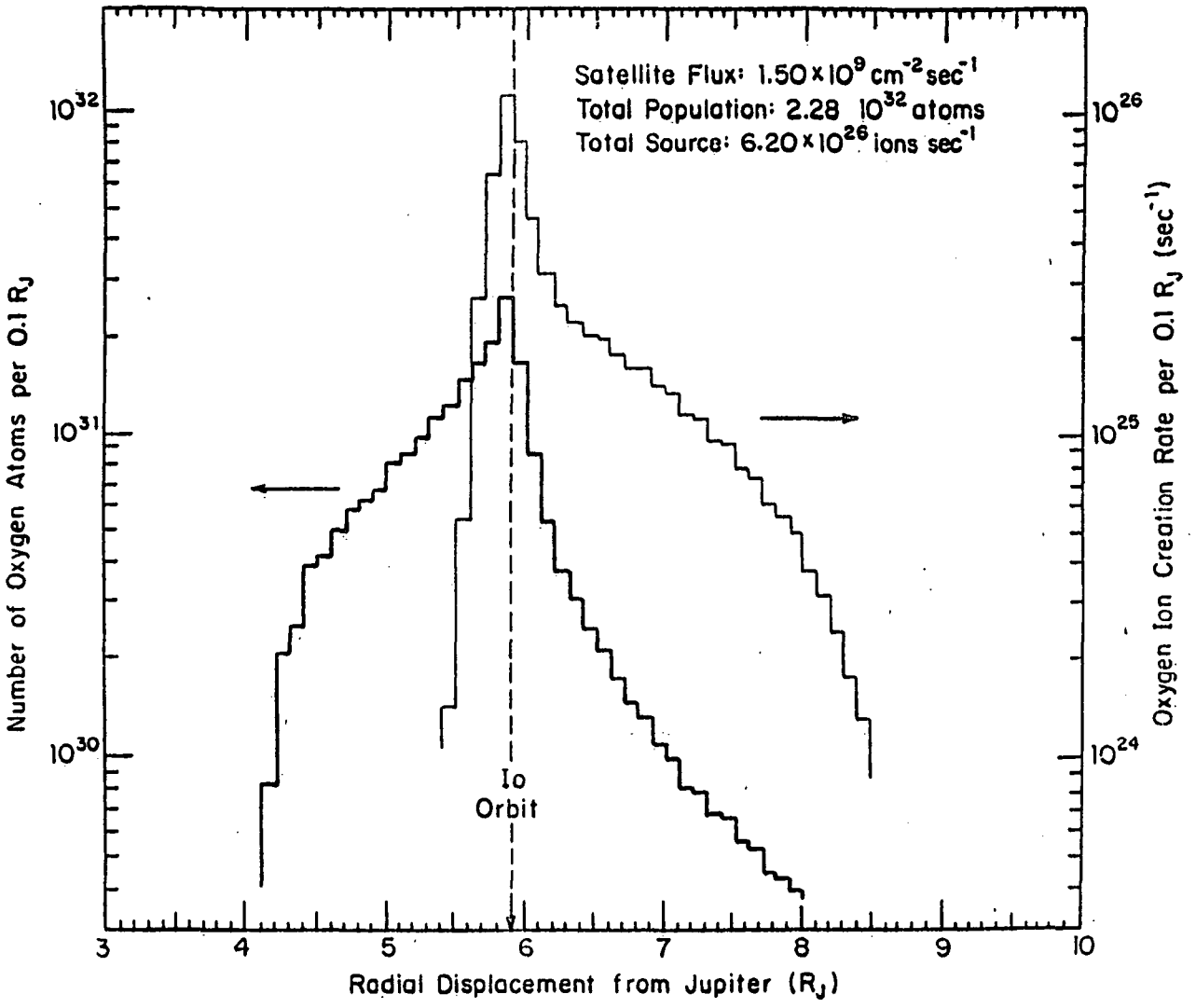
Satellite Flux: 1.50×10^9 cm^-2 sec^-1
Total Population: 2.28 10^32 atoms
Total Source: 6.20×10^26 ions sec^-1
Number of Oxygen Atoms per 0.1 R_J
Oxygen Ion Creation Rate per 0.1 R_J (sec^-1)
10^32
10^31
10^30
10^26
10^25
10^24
Io
Orbit
3
4
5
6
7
8
9
10
Radial Displacement from Jupiter (R_J)

Figure 8